Available online at www.sciencedirect.com
ScienceDirect
Mathematics and Computers in Simulation 182 (2021) 765–790
MATHEMATICS AND COMPUTERS IN SIMULATION
www.elsevier.com/locate/matcom

Original articles

Finite-time event-triggered approach for recurrent neural networks with leakage term and its application

R. Vadivel[a], Porpattama Hammachukiattikul[a], G. Rajchakit[b], M. Syed Ali[c], Bundit Unyong[a,*]

[a] *Department of Mathematics, Faculty of Science and Technology, Phuket Rajabhat University, Phuket, 83000, Thailand*
[b] *Department of Mathematics, Faculty of Science, Maejo University, Chiang Mai, Thailand*
[c] *Department of Mathematics, Thiruvalluvar University, Serkkadu, Vellore 632115, Tamil Nadu, India*

Received 8 April 2020; received in revised form 16 July 2020; accepted 1 December 2020
Available online 9 December 2020

Abstract

This work investigates the finite-time event-triggered approach for recurrent neural networks with leakage term and its application. Here, decentralized event-triggered framework is recommended where event is checked at every sensor node related to local information for available triggering and the updated control is done whenever a centralized event is triggered. By handling the Lyapunov–Krasovskii functional (LKF) method together with novel inequality techniques like Wirtinger single and double integral inequality (WSI,WDI) technique, delay productive term (DPT), and a few adequate conditions are acquired to ensure the finite-time stability (FTS) analysis for the considered system, which is expressed with respect to linear matrix inequalities (LMIs). At last, numerical simulations are provided to indicate the efficiency of the expected results, two of these examples were supported by genuine use of the benchmark issue that correlates with sensible concerns under finite-time execution.

Keywords: Event-triggered; Leakage delay; Lyapunov–Krasovskii functional; Linear matrix inequality; Finite-time stability

1. Introduction

Neural networks (NNs) have gained increased extraordinary consideration due to their potential applications in pattern grouping, remaking of moving image, and combinatorial optimization. Up till now, there are different kinds of NNs namely Hopfield neural network (HNNs) [1], Cellular neural networks [25], Bidirectional associative memory neural networks (BAMNNs) [39], Recurrent neural networks(RNNs) [13] and Cohen–Grossberg neural network (CGNNs) [5], have been employed to solve a variety of practical engineering problems. Although RNNs can be implemented by very large scale integrated circuits, there inevitably exist some delays in neural networks due to the limitation of the speed of transmission and switching of signals [43] and [50]. Meanwhile, time delay is a natural phenomenon frequently experienced in different unique systems, for example, electronic, synthetic systems, long transmission lines in pneumatic systems, organic systems, and moving plant systems. Generally,

* Corresponding author.
E-mail addresses: vadivelsr@yahoo.com (R. Vadivel), bundit.u@pkru.ac.th (B. Unyong).

https://doi.org/10.1016/j.matcom.2020.12.001

delays in NNs may lead oscillation, instability, and divergence, those are all the time in principle sources of terrible efficiency of designed NNs [17,22,31,36,47]. In fact, the stability analysis issue for RNNs with time delays has been an attractive research topic in the previous years, where the time delays under attention can be classified as constant delays, time-varying delays, and distributed delays. Different adequate conditions, either delay-dependent or delay-independent, have been suggested to ensure the stability conditions for the RNNs with time delays, see example [3,12,18,34,37,48].

On the other hand, in recent years, research in the stability analysis of NNs involving leakage term has become more popular and well known in the field of research, since it was broadly explored by numerous researchers in different kinds of NNs. It has been surprising to launch that time delays in leakage terms have an essential impact on the stability issue and dynamical implementation has been destabilized by leakage term for the structured NNs [9,10,16]. Thus, it is clear that, dynamic behaviors of system including leakage, could be developed in the negative input term in the dynamical system, that are outlined back to 1992. Hence, right now, huge number of remarkable research examinations on the dynamical model in account of leakage term can be found in [21]. From that point onward, numerous researchers have been occupied with the assessment of systems over leakage term, therefore many energizing results can be found in different dynamical systems (see, [32,38,45]). As a first attempt, finite-time stability examination for event-triggered communication design to general RNNs and leakage term has been investigated. Recently, in [4], the researchers concentrated on memristive NNs using leakage delay by means of even-triggered control. Also, the authors of [28], the Arcak-type state estimation issue has been talked about for time-delayed static neural networks with leakage delay.

Up to now, enormous results related to stability examination of event-triggered control for various NNs target on various stability issues (e.g, Lyapunov asymptotic (LA) or exponential), that are described through infinite time interval. Not exactly equivalent to the old-style LAS idea, FTS described as the system state omits to overcome a particular bound within the determined finite-time interval [33] and [30]. The introduction of such a stability thought is fundamental and vital in various practical applications, and the appropriate quantities need to fall within the decided limits in a fixed-time interval. Numerous studies regarding event-triggered control with both stability and stabilization in the finite time issues have been accounted in the previous years [24,27,35,41]. For example, in boost converter [20], if the current transformation is too much fast, the circuit will breakdown. Besides, substantial measure of the exceed cannot be associated in various practical engineering [2]. FTS was usually discussed, although finite-time stabilization is still part of the major deal in control theory. Motivated by the above papers, we arranged to structure a finite-time event-triggered control for RNNs. The structure of decentralized event-triggered control is represented in Fig. 1.

Moreover, event-triggered control (ETC) has received increasing interest in the recent years. To moderate the unnecessary waste of computation and communication resources in conventional time-triggered control, ETC has been suggested [6,7,46]. Event-triggered communication design was shown to be a productive method to diminish the transmitted data information in the systems, which can relieve the burden of network bandwidth occupation in comparison with a conventional periodic sampling technique. These days, decentralized event-triggered attracts communication renewed attention because of the appearance of reliable wireless network transmission and low cost microprocessors [29,42,44]. For productive utilization of the limited transmission resources (e.g. battery power and/or network bandwidth), it is natural to introduce event-triggered transmission mechanism into decentralized case execution to decrease some unnecessary transmissions. In [26], centralized and decentralized global outer-synchronizations were achieved by asymmetric recurrent time-varying neural network by data-sampling. Researchers in [49], studied synchronization of master–slave neural networks with a decentralized even triggered communication scheme. Thus, designing the decentralized event-triggered communication scheme is important to save the restricted network resources while ensuring the desired performance. Recently, decentralized event-triggered scheme has received a lot of research interest and some significant results have been published [8,23,40]. To the best of author's knowledge, up to now, decentralized event-triggered communication scheme for RNNs with time-varying delay and leakage terms has never been sufficiently tackled, which despite everything stays an engaging subject in the present research. This encourages the present research work.

According to the above mentioned content, we examine the issue of finite-time event-triggered scheme for RNNs with time-varying delay and leakage terms. The primary contributions are summarized below:

(1) In this work, as a first endeavor, event-triggered control layout is chosen into the RNN model with the time-varying delay and leakage term approach to examine the finite-time stable performance with respect to L–K stability theory.

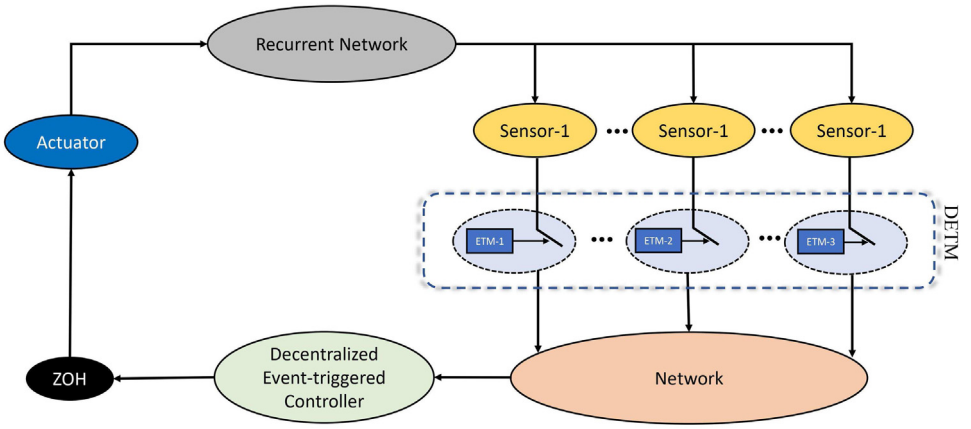

Fig. 1. Outline of conventional decentralized event-triggered case.

(2) In order to reduce the use of constrained communication resources and develop the transmission efficiency, the decentralized event-triggered scheme is presented.
(3) By building a suitable LKF, WSII, WDII, DPT term and recent sufficient conditions assured the considered system is FTS, these are determined on account of LMIs.
(4) To exhibit the genuine application, the quadruple tank process system and circuit system are studied in this work with respect to the RNN model, to demonstrate feasibility on a benchmark issue, which is acknowledged dependent on the finite-time stability achievement.
(5) All the adequate conditions are communicated regarding LMIs which can be tackled by use of MATLAB LMI toolbox. Based on these conditions find out the gain matrices over the constructed ETC.

Notations. A set of fairly standard notations is used in this paper. $\mathbb{N}$ and $\mathbb{R}^n$ mean the positive integers and n-dimensional Euclidean space, respectively. $\mathbb{R}^{n\times m}$ is the arrangement of $n \times m$ real matrices. $X > 0$ ($X \geq 0$) denotes positive definite (semi-positive definite) matrix X; the superscripts T and -1 mean the transpose and inverse of a matrix. $*$ denotes the elements that are introduced due to corresponding symmetry. I means the identity matrix of the appropriate dimensions and diag{...} means the block-diagonal matrix. MAUBs denote the maximum allowable upper bounds. $\lambda_{max}(P)$ or $\lambda_{min}(P)$ denotes the maximum eigenvalue or the minimum eigenvalue of matrix P, respectively.

2. System description and preliminaries

Motivated by the discussions above, we consider the recurrent neural networks (RNNs) with time-varying delay and leakage terms:

$$\begin{cases} \dot{\eta}(t) + D(\eta(t-\sigma)) = W_1 f(\eta(t)) + W_2 f(\eta(t-\rho(t))) + W_3 \int_{t-\rho(t)}^{t} f(\eta(s))ds + u(t), \\ \eta(t) = \phi(t), -\rho \leq t \leq 0 \end{cases} \tag{1}$$

Here $\eta(t) = [\eta_1(t), \eta_2(t), \ldots, \eta_n(t)]^T \in \mathbb{R}^n$ is the neural state vector, $f(\eta(t))$ is the neuron activation function. The matrix $D = diag(d_1, d_2, \ldots, d_n)$ is a diagonal matrix with $d_i > 0$. Interconnection matrices are denoted as W_1, W_2, W_3 and indicate the weight coefficients of the neurons. $u(t) \in \mathbb{R}^n$ is the control input, $\rho(t)$ is the time-varying delay and $\phi(t)$ is the initial condition for $t \in [-d, 0]$, where $d = \max[\sigma, \rho]$. All through this research work, we choose the following assumptions.

Assumption (H1). The activation function fulfills the following condition, there exist constants G_s^- and G_s^+, therefore

$$G_s^- \leq \frac{f_s(\alpha_1) - f_s(\alpha_2)}{\alpha_1 - \alpha_2} \leq G_s^+, \ s = 1, 2, \ldots, n,$$

where $\alpha_1, \alpha_2 \in \mathbb{R}$ and $\alpha_1 \neq \alpha_2$.

Assumption (H2). The constant leakage delay $\sigma > 0$ and time-varying delay $\rho(t)$ satisfy the following conditions:

$$0 \leq \rho(t) \leq \rho, \ \ \dot{\rho}(t) \leq \mu_1, \tag{2}$$

where σ, ρ, and μ_1 are constants.

In the work, both the inputs (n) and measurement faults $\eta(t)$ have been gathered through $\bar{v}$ junction, such that $l \in \{1, 2, \ldots, \bar{v}\}$ has been indicated $\eta_l(t) \in \mathbb{R}^n$ for $\sum_{l=1}^{\bar{v}} n_u = n$. Moreover, the lth event generator discharges moments indicated through $[t_{k_l}^l h]_{K_l}^{\infty} = 0$ and we check the next release $t_{k_l+1}^l h$ of event generator l is controlled by

$$t_{k_l+1}^l h = t_{k_l}^l h + \min_{\tilde{l} \in \ \mathbb{Z}^+} \{\tilde{l}h | r_l^T(t_{k_l}^l h + \tilde{l}h)\hat{\Gamma}_l r_l(t_{k_l}^l h + \tilde{l}h)\} > \hat{\delta}_l \eta_l^T(t_K^l h)\hat{\Gamma}_l \eta_l(t_K^l h), \tag{3}$$

where $t_{k_l}^l h$ is the $k_l th$ transmission time instant of the lth transmitter; $\mathbb{Z}^+$ is denoted as arrangement of positive integers; $\hat{\Gamma}_l > 0$ indicates movable factor to decide the limit of the event-triggered transmitter also, connection among both present sampling vectors, recent communication can be characterized as

$$\eta_l(t_{k_l}^l h + \tilde{l}h) = \eta_l(t_{k_l}^l h + \tilde{l}h) - \eta_l(t_{k_l}^l h).$$

Besides, in (3), above arrangement of $\{t_{k_l}^l h\}$ is a subgroup of $\{0, h, 2h, \ldots\}$. Suppose $\hat{\delta}_l$ is equal to zero, $\{t_{k_l}^l h\}$ are equivalents to $\{0, h, 2h, \ldots\}$. The event-triggered condition in this paper and the sampling are performed independently. In this paper, we are interested in designing the following control input

$$u(t) = K[\eta(t_{k_1}^1 h) \ \ \eta(t_{k_2}^2 h) \ \ldots \ \ \eta(t_{k_n}^n h)]^T, t \in [t_k h, t_{k+1} h), \tag{4}$$

where $K \in \mathbb{R}^{m \times n}$ is to be determined and

$$t_k h = \max_{l=1,2,\ldots,v} \{t_{k_l}^l h\}, \ \ t_{k+1} h = \min_{l=1,2,\ldots,v} \{t_{k_l+1}^l\} h.$$

Let $v_k = t_{k+1} - t_k$. At that point the interval $[t_k h, t_{k+1} h)$ can be communicated as

$$[t_k h, t_{k+1} h) = \bigcup_{j=0}^{v_k - 1} \phi_{\tilde{l}},$$

where $\phi_{\tilde{l}} = [t_k h + \tilde{l}h, t_k h + \tilde{l}h + h)$. Furthermore specified $\phi(t) = t - t_k h - \tilde{l}h$ for $t \in \phi_l$. Obviously $\phi(t)$ is a piecewise-linear function fulfilling

$$\begin{cases} 0 \leq \phi(t) \leq h, & t \in \phi_{\tilde{l}}, \\ \dot{\phi}(t) = 1, & t \neq t_k h + lh. \end{cases} \tag{5}$$

Thus, the threshold error $s_l(t_k h + \tilde{l}h)$ could be revised as

$$\eta_l(t - \phi(t)) = \eta_l(t - \phi(t)) - \eta_l(t_{k_l}^l h), \quad t \in \phi_{\tilde{l}}.$$

Indicate, $r(t - \phi(t)) = col\{r_1(t - \phi(t)), \ r_2(t - \phi(t)) \ , \ldots, \ r_v(t - \phi(t))\}$, such that

$$u(t) = K(\eta(t - \phi(t)) - r(t - \phi(t))), \quad t \in \phi_{\tilde{l}}. \tag{6}$$

Utilizing (6) in (1), we get

$$\begin{aligned} \dot{\eta}(t) = & -D(\eta(t - \sigma)) + W_1 f(\eta(t)) + W_2 f(\eta(t - \rho(t))) + W_3 \int_{t-\rho(t)}^{t} f(\eta(s))ds \\ & + K(\eta(t - \phi(t)) - r(t - \phi(t))), \end{aligned} \tag{7}$$

for $t \in \varphi_{\tilde{l}}$.

Remark 2.1. Based on (3), the following condition holds for $t \in \varphi_{\tilde{l}}$

$$\eta^T(t - \phi(t)) \ \hat{\Gamma} \ r(t - \phi(t)) \leq \hat{\delta}[\eta(t - \phi(t)) - r(t - \phi(t))]^T \hat{\Gamma}[\eta(t - \phi(t)) - r(t - \phi(t))], \tag{8}$$

with $\hat{\Gamma} = diag\{\hat{\Gamma}_1, \hat{\Gamma}_2, \ldots, \hat{\Gamma}_{\tilde{l}}\}$, $\hat{\delta} = diag\{\hat{\delta}_1, \ \hat{\delta}_2, \ldots, \ \hat{\delta}_{\tilde{l}}\}$.

To end this section, some definition and primary lemmas are introduced, which are needed in the main results.

Definition 2.2 ([30]). For a given time $T > 0$, numbers $c_2 > c_1 > 0$, and $\tilde{R}$ is a symmetric positive definite matrix, if there exists control law $K = N_1^{-1}Y$, such that the closed-loop system (7) is finite-time stable in the mean square sense in relation to $(c_1, c_2, T, \tilde{R})$ if the following connection holds:

$$\sup_{-\rho\le s\le 0}\{\phi^T(s)\tilde{R}\phi(s), \dot{\phi}^T(s)\tilde{R}\dot{\phi}(s)\} \le c_1 \Rightarrow \{\eta^T(t)\tilde{R}\eta(t)\} < c_2, \forall t \in [0, T].$$

Lemma 2.3 ([22]). *For $P_7 > 0$ the following inequality holds for all continuously differentiable function $\hat{\eta} \in [a, b] \to \mathbb{R}^n$:*

$$-(b-a)\int_a^b \dot{\hat{\eta}}^T(s)P_7\dot{\hat{\eta}}(s)ds \le -\begin{bmatrix}\tilde{\varrho}_1\\ \tilde{\varrho}_2\end{bmatrix}^T\begin{bmatrix}P_7 & 0\\ * & 3P_7\end{bmatrix}\begin{bmatrix}\tilde{\varrho}_1\\ \tilde{\varrho}_2\end{bmatrix},$$

where $\tilde{\varrho}_1 = \hat{\eta}(b) - \hat{\eta}(a)$, $\tilde{\varrho}_2 = \hat{\eta}(b) + \hat{\eta}(a) - \frac{2}{(b-a)}\int_a^b \hat{\eta}(s)ds$.

Lemma 2.4 ([47]). *Let $\hat{\eta}$ be the differentiable function: $[\upsilon_1,\ \upsilon_2] \to \mathbb{R}^n$ and for symmetric matrices $P_4 > 0$, $\mathscr{M}_i \in \mathbb{R}^{4n\times n}$, the following inequality satisfies:*

$$-\int_{\upsilon_1}^{\upsilon_2}\dot{\hat{\eta}}^T(\theta)P_4\dot{\hat{\eta}}(\theta)d\theta \le \varpi^T\mho\varpi,$$

where $\mho = (\upsilon_2-\upsilon_1)(\mathscr{M}_1P_4^{-1}\mathscr{M}_1^T + 1/3\mathscr{M}_2P_4^{-1}\mathscr{M}_2^T + 1/5\mathscr{M}_3P_4^{-1}\mathscr{M}_3^T) + sym\{\mathscr{M}_1\wp_1 + \mathscr{M}_2\wp_2 + \mathscr{M}_3\wp_3\}$, $\wp_1 = \check{e}_1 - \check{e}_2$, $\wp_2 = \check{e}_1 + \check{e}_2 - 2\check{e}_3$, $\wp_3 = \check{e}_1 - \check{e}_2 - 6\check{e}_3 + 6\check{e}_4$, $\varpi = [\hat{\eta}^T(\upsilon_1)\ \hat{\eta}^T(\upsilon_2)\ \frac{1}{\upsilon_2-\upsilon_1}\int_{\upsilon_1}^{\upsilon_2}\hat{\eta}^T(s)ds\ \frac{2}{(\upsilon_2-\upsilon_1)^2}\int_{\upsilon_1}^{\upsilon_2}\int_{\upsilon_1}^{\theta}\hat{\eta}^T(\theta)d\theta ds]$.

Lemma 2.5 ([36]). *If there exist positive-semi-definite matrices $\mathfrak{G}_{i,j} \in \mathbb{R}^{3n\times 3n}(i, j = 1, \ldots, 3)$, at that point the following connection holds:*

$$-\int_{t-\tau(t)}^{t}\dot{\eta}^T(s)\mathfrak{G}_{33}\dot{\eta}(s)ds \le \int_{t-\tau(t)}^{t}\digamma^T(t)\hbar\digamma(t)dt,$$

where, $\digamma(t) = [\eta^T(t)\ \eta^T(t-\tau(t))\ \dot{\eta}^T(s)]^T$ *and* $\hbar = \begin{bmatrix}\mathfrak{G}_{11} & \mathfrak{G}_{12} & \mathfrak{G}_{13}\\ * & \mathfrak{G}_{22} & \mathfrak{G}_{23}\\ * & * & 0\end{bmatrix}$.

Lemma 2.6 ([31]). *Let $\mathbb{Q} > 0$ be any constant matrix, and for given scalars m and n with $m < n$, the following relation is very much characterized for any differentiable function η in $[m, n] \to \mathbb{R}^n$:*

$$-\frac{n^2-m^2}{2}\int_{-m}^{-n}\int_{t+\theta}^{t}\dot{\eta}^T(s)\mathbb{Q}\dot{\eta}(s)dsd\theta \le -\begin{bmatrix}\delta_a\\ \delta_b\end{bmatrix}^T\begin{bmatrix}\mathbb{Q} & 0\\ * & 2\mathbb{Q}\end{bmatrix}\begin{bmatrix}\delta_a\\ \delta_b\end{bmatrix},$$

where

$$\delta_a = (n-m)\eta(t) - \int_{t-m}^{t-n}\eta(s)ds, \delta_b = \frac{(n-m)}{2}\eta(t) - \int_{t-m}^{t-n}\eta(s)ds + \frac{3}{(n-m)}\int_{-m}^{-n}\int_{t+\theta}^{t}\eta(s)dsd\theta.$$

Moreover, the primary work of this paper is to design event-triggered control for the recurrent neural network model using novel LKF with delay productive type (DPT) term, which is sorted out in the following problem.

Problem 1. Given recurrent neural network (7), achieve finite time stability of the their states $\eta(t)$ under the event triggered controller through the following objectives.
(1) Novel LKF is introduced with the relation of time-varying delay, leakage term and DPT term.
(2) The stabilization conditions with Assumption (H2) are derived which extend the stability region and guarantee the finite time stable performance.

(3) Based on the system (7), both the control gain matrix K and event-triggered parameters $\hat{\Gamma}$ are determined therefore, system attains FTS with respect to Definition 2.2.

3. Main results

In this part, we will firstly give an adequate condition that guarantees the system (7) is finite time stable. Based on the condition, we investigated to design the state feedback controller for event triggered scheme. For presentation convenience, we indicate

$$G_1 = diag\{G_1^- G_1^+,\ G_2^- G_2^+, \ldots,\ G_n^- G_n^+\},\ G_2 = diag\left\{\frac{G_1^- + G_1^+}{2},\ \frac{G_2^- + G_2^+}{2},\ \ldots,\ \frac{G_n^- + G_n^+}{2}\right\},$$

$$e_i = \{0_{n\times(i-1)n}\ I_{n\times n}\ 0_{n\times(20-i)n}\},\ i = 1, 2, \ldots, 20,$$

$$\xi(t) = \Big[\eta^T(t)\ \eta^T(t-\sigma)\ \int_{t-\sigma}^{t}\eta^T(s)ds\ \eta^T(t-\rho(t))\ \eta^T(t-\rho)\ f^T(\eta(t))\ f^T(\eta(t-\rho(t)))\ \int_{t-\rho(t)}^{t}\eta(s)ds$$
$$\int_{t-\rho}^{t-\rho(t)}\eta(s)ds\int_{t-\rho}^{t}f^T(\eta(s))ds\ \int_{-\rho(t)}^{0}\int_{t+\theta}^{t}\eta^T(s)dsd\theta\int_{-\rho}^{-\rho(t)}\int_{t+\theta}^{t}\eta^T(s)dsd\theta\ \int_{t-\rho}^{t}\eta(s)ds$$
$$\int_{t-\rho}^{t}\int_{t+\theta}^{t}\eta^T(s)dsd\theta\ \eta^T(t-\phi(t))\ \eta^T(t-h)\ \int_{t-\phi(t)}^{t}\eta(s)ds\ \int_{t-h}^{t-\rho(t)}\eta(s)ds\ r^T(t-\phi(t))\ \dot{\eta}(t)\Big],$$

$$\tilde{\gamma}_1 = \eta(t) - \eta(t-\rho(t)),\ \tilde{\gamma}_2 = \eta(t) + \eta(t-\rho(t)) - \frac{2}{\rho(t)}\int_{t-\rho(t)}^{t}\eta^T(s)ds,$$

$$\tilde{\gamma}_3 = \eta(t) - \eta(t-\rho(t)) - \frac{6}{\rho(t)}\int_{t-\rho(t)}^{t}\eta^T(s)ds + \frac{6}{\rho^2(t)}\int_{-\rho(t)}^{0}\int_{t+\theta}^{t}\eta^T(s)dsd\theta,$$

$$\tilde{\gamma}_4 = \eta(t-\rho(t)) - \eta(t-\rho),\ \tilde{\gamma}_5 = \eta(t-\rho(t)) + \eta(t-\rho) - \frac{2}{(\rho(t)-\rho)}\int_{t-\rho}^{t-\rho(t)}\eta^T(s)ds,$$

$$\tilde{\gamma}_6 = \eta(t) - \eta(t-\rho(t)) - \frac{6}{(\rho(t)-\rho)}\int_{t-\rho}^{t-\rho(t)}\eta^T(s)ds + \frac{6}{(\rho(t)-\rho)^2}\int_{-\rho}^{-\rho(t)}\int_{t+\theta}^{t}\eta^T(s)dsd\theta,$$

$$\gamma_1 = \lambda_{\min}(P),$$

$$\gamma_2 = 2\lambda_{\max}(R^{-1/2}PR^{-1/2}) + 2\sigma^2\lambda_{\max}(D^TR^{-1/2}PR^{-1/2}D) + \sigma\lambda_{\max}(R^{-1/2}P_1R^{-1/2})$$
$$+ \frac{\sigma^3}{2}\lambda_{\max}(R^{-1/2}P_2R^{-1/2}) + \rho\lambda_{\max}(R^{-1/2}P_3R^{-1/2}) + \rho\lambda_{\max}(R^{-1/2}R_1R^{-1/2})$$
$$+ \frac{\rho^3}{2}\lambda_{\max}(R^{-1/2}P_4R^{-1/2}) + \frac{\rho^3}{2}\lambda_{\max}(R^{-1/2}R_2R^{-1/2}) + \rho\lambda_{\max}(R^{-1/2}Q_1R^{-1/2})$$
$$+ h\lambda_{\max}(R^{-1/2}P_6R^{-1/2}) + \frac{h^3}{2}\lambda_{\max}(R^{-1/2}P_7R^{-1/2}) + \frac{\rho^5}{2}\lambda_{\max}(R^{-1/2}P_8R^{-1/2}),$$

$$\gamma_3 = 2\lambda_{\max}(P) + 2\sigma^2\lambda_{\max}(D^TPD) + \sigma\lambda_{\max}(P_1) + \frac{\sigma^3}{2}\lambda_{\max}(P_2) + \rho\lambda_{\max}(P_3) + \rho\lambda_{\max}(R_1)$$
$$+ \frac{\rho^3}{2}\lambda_{\max}(P_4) + \frac{\rho^3}{2}\lambda_{\max}(R_2) + \rho\lambda_{\max}(Q_1) + h\lambda_{\max}(P_6) + \frac{h^3}{2}\lambda_{\max}(P_7) + \frac{\rho^5}{2}\lambda_{\max}(P_8),$$

$$\hat{\phi}_1 = [e_1\ e_5\ \frac{1}{\rho(t)}e_8\ \frac{1}{\rho^2(t)}e_{11}],\ \hat{\phi}_2 = [e_4\ e_5\ \frac{1}{\rho(t)}e_9\ \frac{1}{\rho^2(t)}e_{12}],\ \wp_1 = P_4 - A_{33},\ \wp_2 = P_4 - B_{33}.$$

Theorem 3.1. *For scalars σ, ρ, μ_1 and h the recurrent neural networks expressed by (1) are FTS in the mean square sense for both time-varying delay signals $\rho(t)$ and $\phi(t)$ fulfilling (2), if there exist matrices $P > 0, P_i > 0 (i = 1, 2, 3, 4, 6, 7, 8), R_1 > 0, R_2 > 0, Q_1 > 0, V_1 > 0, Y > 0, N_1 > 0, \hat{\Gamma} > 0$, any matrices $\mathcal{N} \in \mathbb{R}^{3n\times n}$, positive diagonal matrices $\beta_l > 0$, $(l = 1, 2)$ and semi positive definite matrices $A, B \in \mathbb{R}^{3n\times 3n}$, so as the following*

inequalities hold:

$$\Psi = \begin{bmatrix} \sum_{i=1}^{8} \Phi_i & \hat{\Upsilon} \\ * & \hat{\Omega} \end{bmatrix} < 0, \tag{9}$$

$$2\gamma_2 c_1 \lambda_{\max}\{\tilde{R}\}\left[\frac{\sigma\lambda_{\max}\{D^2\}}{\lambda_{\min}\{P_2\}} + \frac{e^{\alpha t}}{\gamma_1}\right] \le c_2, \tag{10}$$

where

$$\begin{aligned}
\Phi_1 &= 2[e_1 - De_3]Pe_{20}^T + e_1(W_1 - W_2)\chi_1 e_{20}^T + e_6(\chi_1 - \chi_2)e_{20}^T,\\
\Phi_2 &= e_1P_1e_1^T - e_5P_1e_5^T + \sigma^2 e_1P_2e_1^T - e_3P_2e_3^T,\\
\Phi_3 &= e_1(P_3 + Q_1)e_1^T - e_4P_3e_4^T c - e_5Q_1e_5^T - \rho^2 e_{20}P_4e_{20}^T + e_6(R_1 + \rho^2R_2)e_6^T\\
&\quad - (1-\mu_1)e_7R_1e_7^T + sym\{\mathscr{N}_1\tilde{\gamma}_1 + \mathscr{N}_2\tilde{\gamma}_2 + \mathscr{N}_3\tilde{\gamma}_3\} + sym\{\mathscr{N}_1\tilde{\gamma}_4 + \mathscr{N}_2\tilde{\gamma}_5 + \mathscr{N}_3\tilde{\gamma}_6\} + \Phi_{33},\\
\Phi_4 &= e_1P_6e_1^T + h^2 e_{20}P_7e_{20}^T + \hat{\Pi}_3^T(t)\Omega_2\hat{\Pi}_3(t) + \hat{\Pi}_4^T(t)\Omega_2\hat{\Pi}_4(t),\\
\Phi_5 &= \frac{\rho^4}{4}e_{20}P_8e_{20}^T - \Xi_1^T\begin{bmatrix} P_8 & 0 \\ * & 2P_8 \end{bmatrix}\Xi_1,\\
\Phi_6 &= \rho(e_1V_1e_1^T - e_5V_1e_5^T) - 2(e_1 - e_5)V_1(e_8^T + e_9^T),\\
\Phi_7 &= 2[e_1N_1 + e_{20}N_1][-e_{20}^T + De_2^T + W_1e_6^T + W_2e_7^T + W_3e_{10}^T]\\
&\quad + [e_1Le_{15}^T - e_1Le_{19}^T + e_{15}Le_{20}^T - e_{19}L^Te_{20}^T],\\
\Phi_8 &= \hat{\delta}[e_{15} - e_{19}]\tilde{\Gamma}[e_{15} - e_{19}]^T - e_{15}\tilde{\Gamma}e_{19}^T,\\
\hat{\Upsilon} &= \{\hat{\Upsilon}_1\ \ \hat{\Upsilon}_2\},\ \ \hat{\Omega} = \{\hat{\Omega}_1,\ \ \hat{\Omega}_2\},\ \ \hat{\Omega}_1 = \hat{\Omega}_2 = diag\{-\wp_i \quad -3\wp_i \quad -5\wp_i\}, i = 1,2,\\
\hat{\Upsilon}_1 &= [\sqrt{\rho(t)}\hat{\phi}_1\mathscr{N}_1 \quad \sqrt{\rho(t)}\hat{\phi}_1\mathscr{N}_2 \quad \sqrt{\rho(t)}\hat{\phi}_1\mathscr{N}_3],\\
\hat{\Upsilon}_2 &= [\sqrt{(\rho-\rho(t))}\hat{\phi}_2\mathscr{N}_4 \quad \sqrt{(\rho-\rho(t))}\hat{\phi}_2\mathscr{N}_5 \quad \sqrt{(\rho-\rho(t))}\hat{\phi}_2\mathscr{N}_6],\\
W_1 &= diag\{W_1^+,\ W_2^+, \ldots,\ W_n^+\},\ W_2 = diag\{W_1^-,\ W_2^-, \ldots,\ W_n^-\},\\
\Phi_{33} &= e_1(\rho(t)A_{11} + 2A_{13})e_1^T + 2e_1(\rho(t)A_{12} - A_{13} + A_{23}^T)e_4^T + e_4(\rho(t)A_{22} - 2A_{23})e_4^T\\
&\quad + e_4((\rho-\rho(t))B_{11} + 2B_{13})e_4^T + 2e_4((\rho-\rho(t))B_{12} - B_{13} + B_{23}^T)e_5^T\\
&\quad + e_5((\rho-\rho(t))B_{22} - 2B_{23})e_5^T + \begin{bmatrix} e_1 \\ e_6 \end{bmatrix}^T\begin{bmatrix} -G_1\beta_1 & G_2\beta_1 \\ * & -\beta_1 \end{bmatrix}\begin{bmatrix} e_1 \\ e_6 \end{bmatrix}^T\\
&\quad + \begin{bmatrix} e_4 \\ e_7 \end{bmatrix}^T\begin{bmatrix} -G_1\beta_2 & G_2\beta_2 \\ * & -\beta_2 \end{bmatrix}\begin{bmatrix} e_4 \\ e_7 \end{bmatrix}^T.
\end{aligned}$$

Furthermore, the feedback gain K in (6) *could be chosen by* $K = N_1^{-1}Y$

Proof. We select the appropriate L–K functional:

$$V(t) = \sum_{r=1}^{5} V_r(t) + \tilde{V}(t), \tag{11}$$

where

$$\begin{aligned}
V_1(t) &= e^{\alpha t}\Big[[\eta(t) - D\int_{t-\sigma}^{t}\eta(s)ds]^T P[\eta(t) - D\int_{t-\sigma}^{t}\eta(s)ds]\\
&\quad + 2\sum_{i=1}^{n}\int_0^{\eta_i(t)}[\nu_{1i}(W_i^+(s) - f_i(s)) + \nu_{2i}(f_i(s) - W_i(s))]ds\Big],\\
V_2(t) &= e^{\alpha t}[\int_{t-\sigma}^{t}\eta^T(s)P_1\eta(s)ds + \sigma\int_{-\sigma}^{0}\int_{t+\theta}^{t}\eta^T(s)P_2\eta(s)dsd\theta],
\end{aligned}$$

$$V_3(t) = e^{\alpha t}[\int_{t-\rho(t)}^{t}[\eta^T(s)P_3\eta(s) + f^T(\eta(s))R_1 f(\eta(s))]ds + \rho\int_{-\rho}^{0}\int_{t+\theta}^{t}[\dot{\eta}^T(s)P_4\dot{\eta}(s) + f^T(\eta(s))R_2 f(\eta(s))]dsd\theta + \int_{t-\rho}^{t}\eta^T(s)Q_1\eta(s)ds],$$

$$V_4(t) = e^{\alpha t}[\int_{t-\phi(t)}^{t}\eta^T(s)P_6\eta(s)ds + h\int_{-h}^{0}\int_{t+\theta}^{t}\dot{\eta}^T(s)P_7\dot{\eta}(s)dsd\theta],$$

$$V_5(t) = e^{\alpha t}[\frac{\rho^2}{2}\int_{-\rho}^{0}\int_{\theta}^{0}\int_{t+\lambda}^{t}\dot{\eta}^T(s)P_8\dot{\eta}(s)dsd\lambda d\theta],$$

$$\tilde{V}(t) = e^{\alpha t}[\rho\int_{t-\rho}^{t}\eta^T(s)V_1\eta(s)ds - \int_{t-\rho}^{t}\eta^T(s)ds V_1\int_{t-\rho}^{t}\eta(s)ds].$$

Calculating the time derivative of $V_i(t)(i = 1, 2, 3, 4, 5)$, we get

$$\begin{aligned}\dot{V}_1(t) &= 2e^{\alpha t}[[\eta(t) - D\int_{t-\sigma}^{t}\eta(s)ds]^T P\dot{\eta}(t) + \eta^T(t)(W_1 - W_2)\chi_1\dot{\eta}(t) + f^T(\eta(t))(\chi_1 - \chi_2)\dot{\eta}(t)] + \alpha V_1(t)\\ &= e^{\alpha t}[\zeta^T(t)\Phi_1\zeta(t)] + \alpha V_1(t), \qquad (12)\\ \dot{V}_2(t) &= e^{\alpha t}[\eta^T(t)P_1\eta(t) - \eta^T(t-\sigma)P_1\eta(t-\sigma) + \eta^T(t)\sigma^2 P_2\eta(t) - \sigma\int_{t-\sigma}^{t}\eta^T(s)P_2\eta(t)] + \alpha V_2(t)\\ &\le e^{\alpha t}[\zeta^T(t)\Phi_2\zeta(t)] + \alpha V_2(t), \qquad (13)\\ \dot{V}_3(t) &\le e^{\alpha t}[\eta^T(t)P_3\eta(t) - \eta(t-\rho(t))P_3\eta(t-\rho(t)) + \eta^T(t)Q_1\eta(t) - \eta^T(t-\rho)Q_1\eta(t-\rho)\\ &\quad - \rho^2\dot{\eta}^T(t)P_4\dot{\eta}(t) - \rho\int_{t-\rho}^{t}\dot{\eta}^T(s)P_4\dot{\eta}(s)ds + f^T(\eta(t))R_1 f(\eta(t))\\ &\quad - (1-\mu_1)f^T(\eta(t-\rho(t)))R_1 f(\eta(t-\rho(t))) + \rho^2 f^T(\eta(t))R_2 f(\eta(t))\\ &\quad - \rho\int_{t-\rho}^{t}f^T(\eta(s))R_2 f(\eta(s))ds] + \alpha V_3(t),\\ &\le e^{\alpha t}[\zeta^T(t)\{\Phi_3 + \Phi_{22} + \Phi_{33}\}\zeta(t)] + \alpha V_3(t), \qquad (14)\\ \dot{V}_4(t) &\le e^{\alpha t}[\eta^T(t)P_6\eta(t) + h^2\dot{\eta}^T(t)P_7\dot{\eta}(t)ds - h\int_{t-h}^{t}\dot{\eta}^T(s)P_7\dot{\eta}(s)ds] + \alpha V_4(t),\\ &\le e^{\alpha t}[\zeta^T(t)\{e_1 P_6 e_1^T + h^2 e_{20}P_7 e_{20}^T + \hat{\Pi}_3^T(t)\Omega_2\hat{\Pi}_3(t) + \hat{\Pi}_4^T(t)\Omega_2\hat{\Pi}_4(t)\}\zeta(t)] + \alpha V_4(t),\\ &\le e^{\alpha t}[\zeta^T(t)\Phi_4\zeta(t)] + \alpha V_4(t) \qquad (15)\end{aligned}$$

and

$$\begin{aligned}\dot{\tilde{V}}(t) &= e^{\alpha t}[\rho(\eta^T(t)V_1\eta(t) - \eta^T(t-\rho)V_1\eta(t-\rho)) - 2((\eta^T(t) - \eta(t-\rho))V_1(\int_{t-\rho(t)}^{t}\eta^T(s)ds\\ &\quad + \int_{t-\rho}^{t-\rho(t)}\eta^T(s)ds))] + \alpha\tilde{V}(t),\\ &= e^{\alpha t}[\zeta^T(t)\Phi_6\zeta(t)] + \alpha\tilde{V}(t). \qquad (16)\end{aligned}$$

By Lemma 2.6, we obtain

$$\begin{aligned}\dot{V}_5(t) &= e^{\alpha t}[\frac{\rho^4}{4}\dot{\eta}^T(t)P_8\dot{\eta}(t) - \frac{\rho^2}{2}\int_{-\rho}^{0}\int_{t+\theta}^{t}\dot{\eta}^T(s)P_8\dot{\eta}(s)dsd\theta] + \alpha V_5(t)\\ &\le e^{\alpha t}[\frac{\rho^4}{4}\dot{\eta}^T(t)P_8\dot{\eta}(t) - \Xi_1^T\begin{bmatrix}P_8 & 0\\ * & 2P_8\end{bmatrix}\Xi_1] + \alpha V_5(t),\\ &\le e^{\alpha t}[\zeta^T(t)\Phi_5\zeta(t)] + \alpha V_5(t), \qquad (17)\end{aligned}$$

where $\Xi_1 = \begin{bmatrix}\rho\eta(t) - \rho\tilde{\gamma}_1(t)\\ \frac{\rho}{2}\eta(t) - \rho\tilde{\gamma}_1(t) + \tilde{\gamma}_2(t)\end{bmatrix}$, $\tilde{\gamma}_1(t) = \int_{t-\rho}^{t}\eta(s)ds$, $\tilde{\gamma}_2(t) = \frac{3}{\rho}\int_{t-\rho}^{t}\int_{t+\theta}^{t}\eta(s)dsd\theta$.

Using Jensen's inequality the integral terms in (13) and (14), can be written as

$$-\sigma\int_{t-\sigma}^{t}\eta^T(s)P_2\eta(t)\leq\left(\int_{t-\sigma}^{t}\eta(s)ds\right)^T P_2\left(\int_{t-\sigma}^{t}\eta(s)ds\right)$$
$$-\rho\int_{t-\rho}^{t}f^T(\eta(s))R_2f(\eta(s))ds\leq\left(\int_{t-\rho}^{t}f(\eta(s))ds\right)^T R_2\left(\int_{t-\rho}^{t}f(\eta(s))ds\right).$$

Since $0\leq\rho(t)\leq\rho$, the integral term in (14) can be written in the following aspects:

$$-\int_{t-\rho}^{t}\dot\eta^T(s)P_4\dot\eta(s)ds=-\int_{t-\rho(t)}^{t}\dot\eta^T(s)P_4\dot\eta(s)ds-\int_{t-\rho}^{t-\rho(t)}\dot\eta^T(s)P_4\dot\eta(s)ds, \tag{18}$$

Utilizing Lemmas 2.4 and 2.5, the following inequality holds:

$$\begin{aligned}-\int_{t-\rho(t)}^{t}\dot\eta^T(s)P_4\dot\eta(s)ds-\int_{t-\rho}^{t-\rho(t)}\dot\eta^T(s)P_4\dot\eta(s)ds&\\
\leq-\int_{t-\rho(t)}^{t}\dot\eta^T(s)\{P_4-A_{33}\}\dot\eta(s)ds-\int_{t-\rho}^{t-\rho(t)}\dot\eta^T(s)\{P_4-B_{33}\}\dot\eta(s)ds,&\\
\leq\zeta^T(t)\{\hat\phi_1[\rho(t)\mathcal{N}_1\{P_4-A_{33}\}\mathcal{N}_1^T+\frac{\rho(t)}{3}\mathcal{N}_2\{P_4-A_{33}\}\mathcal{N}_2^T&\\
+\frac{\rho(t)}{5}\mathcal{N}_3\{P_4-A_{33}\}\mathcal{N}_3^T]^T\hat\phi_1^T+sym\{\mathcal{N}_1\tilde\gamma_1+\mathcal{N}_2\tilde\gamma_2+\mathcal{N}_3\tilde\gamma_3\}&\\
+\hat\phi_2[(\rho-\rho(t))\mathcal{N}_1\{P_4-B_{33}\}\mathcal{N}_1^T+\frac{(\rho-\rho(t))}{3}\mathcal{N}_2\{P_4-B_{33}\}\mathcal{N}_2^T&\\
+\frac{(\rho-\rho(t))}{5}\mathcal{N}_3\{P_4-B_{33}\}\mathcal{N}_3^T]^T\hat\phi_2^T+sym\{\mathcal{N}_1\tilde\gamma_4+\mathcal{N}_2\tilde\gamma_5+\mathcal{N}_3\tilde\gamma_6\}\}\zeta(t),&\\
\leq\zeta^T(t)\Phi_{22}\zeta(t).&\end{aligned} \tag{19}$$

Employing Lemma 2.5 and Leibniz–Newton formula, we obtain the subsequent inequality

$$\begin{aligned}-\int_{t-\rho(t)}^{t}\dot\eta^T(s)A_{33}\dot\eta(s)ds-\int_{t-\rho}^{t-\rho(t)}\dot\eta^T(s)B_{33}\dot\eta(s)ds&\leq\eta^T(t)(\rho(t)A_{11}+2A_{13})\eta(t)\\
+2\eta^T(t)(\rho(t)A_{12}-A_{13}+A_{23}^T)\eta(t-\rho(t))&\\
+\eta(t-\rho(t))(\rho(t)A_{22}-2A_{23})\eta^T(t-\rho(t))&\\
+\eta^T(t-\rho(t))((\rho-\rho(t))B_{11}+2B_{13})\eta(t-\rho(t))&\\
+2\eta^T(t-\rho(t))((\rho-\rho(t))B_{12}-B_{13}+B_{23}^T)\eta(t-\rho)&\\
+\eta(t-\rho)((\rho-\rho(t))B_{22}-2B_{23})\eta^T(t-\rho),&\\
\leq\zeta^T(t)\Phi_{33}\zeta(t).&\end{aligned}$$

Moreover, by using Lemma 2.3 and $P_7>0$, the following inequality is obtained:

$$\begin{aligned}-\int_{t-h}^{t}\dot\eta^T(s)P_7\dot\eta(s)ds&=-\int_{t-\phi(t)}^{t}\dot\eta^T(s)P_7\dot\eta(s)ds-\int_{t-h}^{t-\phi(t)}\dot\eta^T(s)P_7\dot\eta(s)ds,\\
&\leq-\zeta^T(t)[\hat\Pi_3^T(t)\Omega_2\hat\Pi_3(t)+\hat\Pi_4^T(t)\Omega_2\hat\Pi_4(t)]\zeta(t),\end{aligned}$$

where $\hat\Pi_3(t)=\begin{bmatrix}e_1-e_{15}\\ e_1+e_{15}-\frac{2}{\phi(t)}e_{17}\end{bmatrix}$, $\hat\Pi_3(t)=\begin{bmatrix}e_{15}-e_{16}\\ e_{15}+e_{16}-\frac{2}{h-\phi(t)}e_{18}\end{bmatrix}$, $\Omega_2=\begin{bmatrix}P_7&0\\ *&3P_7\end{bmatrix}$.

In addition, for any dimensioned diagonal matrix $\beta_i>0, i=1,2$, we obtain from Assumption (H1)

$$\begin{aligned}0&\leq\begin{bmatrix}\eta(t)\\ f(\eta(t))\end{bmatrix}^T\begin{bmatrix}-G_1\beta_1&G_2\beta_1\\ *&-\beta_1\end{bmatrix}\begin{bmatrix}\eta(t)\\ f(\eta(t))\end{bmatrix},\\
0&\leq\begin{bmatrix}\eta(t-\rho(t))\\ f(\eta(t-\rho(t)))\end{bmatrix}^T\begin{bmatrix}-G_1\beta_2&G_2\beta_2\\ *&-\beta_2\end{bmatrix}\begin{bmatrix}\eta(t-\rho(t))\\ f(\eta(t-\rho(t)))\end{bmatrix},\end{aligned} \tag{20}$$

Note that, for any suitable dimensioned matrix N_1 the subsequent zero equation holds:

$$2\Big[\eta^T(t)N_1+\dot{\eta}^T(t)N_1\Big]\Big[-\dot{\eta}(t)-D(\eta(t-\sigma))+W_1f(\eta(t))+W_2f(\eta(t-\rho(t)))+W_3\int_{t-\rho(t)}^{t}f(\eta(s))ds+K(\eta(t-\phi(t))-s(t-\phi(t)))\Big]e^{\alpha t}=0,$$
$$2e^{\alpha t}\{\zeta^T(t)\Phi_7\zeta(t)\}=0. \tag{21}$$

Combining (12)–(21) with (8), we get

$$\dot{V}(t)\leq\alpha V(t)+e^{\alpha t}[\xi(t)^T\Psi\xi(t)], \tag{22}$$

From (9), we get the following inequality

$$\dot{V}(t)\leq\alpha V(t), \tag{23}$$

By multiplying $e^{-\alpha t}$ on both sides of (23), we get

$$e^{-\alpha t}\dot{V}(t)\leq e^{-\alpha t}\alpha V(t),$$
$$e^{-\alpha t}\dot{V}(t)-\alpha e^{-\alpha t}V(t)<0. \tag{24}$$

Taking integration of the above inequality on both sides from 0 to t, we get

$$e^{-\alpha t}V(t)-V(0)\leq 0. \tag{25}$$

Moreover, from the definition of $V(t)$ gives

$$\begin{aligned}V(t)&\geq e^{\alpha t}[\eta(t)-D\int_{t-\sigma}^{t}\eta(s)ds]^TP[\eta(t)-D\int_{t-\sigma}^{t}\eta(s)ds]\\&\geq\lambda_{\min}(P)e^{\alpha t}[\eta(t)-D\int_{t-\sigma}^{t}\eta(s)ds]^T[\eta(t)-D\int_{t-\sigma}^{t}\eta(s)ds]\\&\geq\lambda_{\min}(P)\|\eta(t)-D\int_{t-\sigma}^{t}\eta(s)ds\|^2.\end{aligned} \tag{26}$$

Moreover,

$$\begin{aligned}\|\eta(t)-D\int_{t-\sigma}^{t}\eta(s)ds\|^2&\leq\lambda_{\max}(D^2)(\int_{t-\sigma}^{t}\eta^T(s)ds)(\int_{t-\sigma}^{t}\eta(s)ds)\\&\leq\sigma\frac{\lambda_{\max}(D^2)}{\lambda_{\min}(P_2)}e^{-\alpha t}\{e^{\alpha t}(\int_{t-\sigma}^{t}\eta^T(s)P_2\eta(s)ds)\}\\&\leq\sigma\frac{\lambda_{\max}(D^2)}{\lambda_{\min}(P_2)}e^{-\alpha t}\{e^{\alpha t}V(0)\}\\&\leq\sigma\frac{\lambda_{\max}(D^2)}{\lambda_{\min}(P_2)}\{V(0)\}.\end{aligned} \tag{27}$$

Here,

$$V(0)\leq\gamma_2\sup_{-\rho^*\leq s\leq 0}\{\tilde{\phi}^T(s)\tilde{R}\tilde{\phi}(s),\ \dot{\tilde{\phi}}^T(s)\tilde{R}\dot{\tilde{\phi}}(s)\}\leq\gamma_2c_1,$$
$$V(0)\leq\gamma_3\|\tilde{\phi}\|^2 \tag{28}$$

where γ_2 and γ_3 are defined in Theorem 3.1. Therefore from (25) and (26), we get

$$e^{-\alpha t}V(t)\leq V(0)$$
$$e^{-\alpha t}\{\lambda_{\min}(P)\|\eta(t)-A\int_{t-\sigma}^{t}\eta(s)ds\|^2\}\leq e^{-\alpha t}V(t)\leq V(0)\leq\gamma_2c_1. \tag{29}$$

Moreover,

$$\|\eta(t)\|^2=2\|D\int_{t-\sigma}^{t}\eta(s)ds\|^2+2\|\eta(t)-D\int_{t-\sigma}^{t}\eta(s)ds\|^2.$$

From (27)–(29), we get

$$\eta^T(t)\eta(t) \leq 2\gamma_2 c_1\left(\sigma\frac{\lambda_{\max}(D^2)}{\lambda_{\min}(P_2)} + \frac{e^{\alpha t}}{\lambda_{\min}(P)}\right),$$
$$\eta^T(t)\tilde{R}\eta(t) \leq 2\gamma_2 c_1\lambda_{\min}(\tilde{R})\left(\sigma\frac{\lambda_{\max}(D^2)}{\lambda_{\min}(P_2)} + \frac{e^{\alpha t}}{\lambda_{\min}(P)}\right),$$
$$\eta^T(t)\tilde{R}\eta(t) \leq c_2. \tag{30}$$

Hence the proof.

Remark 3.2. We deal with the subsequent system, as an appropriate instance of the system (7) reduced to delayed NNs with leakage term and can be described as

$$\dot{\eta}(t) = -D(\eta(t-\sigma)) + W_1 f(\eta(t)) + W_2 f(\eta(t-\rho(t))). \tag{31}$$

Finite time stable results for neural networks (31) can be achieved in Corollary 3.3:

Corollary 3.3. *For given σ, ρ, μ_1, the system (31) is FTS in the mean square sense for any time-varying delay signals $\rho(t)$ fulfilling (2), if there exist matrices $P > 0$, $P_i > 0 (i = 1, 2, 3, 4, 8)$, $R_1 > 0$, $R_2 > 0$, $Q_1 > 0$, $V_1 > 0$, any matrices $\mathcal{N}_i$, $(i = 1, 2, \ldots, 6)$, positive diagonal matrices $\beta_l > 0$, $(l = 1, 2)$ and semi positive definite matrices $A, B \in \mathbb{R}^{3n\times 3n}$ so that the subsequent LMIs hold:*

$$\begin{bmatrix} \sum_{i=1}^{3}\Phi_i + \sum_{i=5}^{7}\Phi_i & \hat{\Upsilon} \\ * & \hat{\Omega} \end{bmatrix} < 0, \tag{32}$$

$$2\gamma_2 c_1\lambda_{\max}\{\tilde{R}\}\left[\frac{\sigma\lambda_{\max}\{D^2\}}{\lambda_{\min}\{P_2\}} + \frac{e^{\alpha t}}{\gamma_1}\right] \leq c_2. \tag{33}$$

Proof. Let $P_6 = P_7 = 0$ in Theorem 3.1, we get the finite time stability criterion for system (31). The proof is like that of Theorem 3.1. Hence it is excluded.

Remark 3.4. In order to save the limited communication resources, we introduce the decentralized event-triggered scheme for recurrent neural networks. It is important to note that very limited works have been done on event-triggered scheme with leakage terms under the finite-time stability (FTS) condition. More particularly, several results have been reported on event-triggered design for various types on NNs like Markovian jumping NNs [6], memristor NNs [7], complex valued NNs [42,44], and switched NNs [46]. The model considered in the present study is more practical than that proposed by [6,7,42,44,46], because they did not consider finite-time event-triggered recurrent neural networks (FTETRNNs) with leakage terms. It should be noted that, the criteria proposed in these researches are restricted to analyzing the finite-time stability of NNs based on control techniques. Moreover, finite-time stability differs from asymptotic stability, which admits that the state does not exceed a certain bound during a fixed finite-time interval. Based on this scenario, this paper addressed the FTS problem of RNNs subject to decentralized event-triggered communication, limited network-bandwidth, and leakage delay. Notably, the implementation of decentralized event-triggered scheme improved the performance of the system and also minimized the network transmissions. Hence, the analysis technique and system model proposed in this paper deserve much attention to fill such demands more effectively.

Remark 3.5. Based on the results considered in [24,27,41], the feedback control established for ensuring the stabilization in the sense on FTS of System (1) cannot be developed with the presence of a leakage delay. The LMIs conditions presented in these researches are not in the form of LMIs when $\sigma \neq 0$ which renders the control algorithm more difficult. To solve the previously mentioned issue, the matrix K should be in the accompanying structure $K = N_1^{-1}Y$. With this type of K, it is easy to find LMI conditions ready to guarantee the FTS of RNNs in the previously mentioned articles, even a leakage delay is available.

Remark 3.6. Primarily, computational complexity will be a major issue dependent on how big are the LMIs and how more are the decision variables. However, big size of LMIs yields better execution. The results in Theorem 3.1

Table 1
MAUB ρ for various values $\dot{\rho}(t)$ and σ in Example 4.1.

μ_1	0.1	0.3	0.5	0.7	0.8
$\sigma = 0.05$	5.7251	5.3472	5.1203	4.9015	4.8731
$\sigma = 0.1$	4.7861	4.7310	4.5681	4.4503	4.3173
$\sigma = 0.15$	4.2723	4.1205	3.9672	3.8521	3.6501
$\sigma = 0.2$	3.5251	3.2603	3.1752	2.9854	2.7982
$\sigma = 0.25$	Infeasible	Infeasible	Infeasible	Infeasible	Infeasible

Table 2
MABs ρ for various values μ_1 in Example 4.4.

μ_1	0.1	0.5	0.9	NODV's
[12]	3.2793	2.2245	1.5847	$12.5n^2 + 5.5n$
[43]	3.4886	2.6056	2.2522	$7.5n^2 + 5.5n$
[18]	3.7857	3.0546	2.6703	$30.5n^2 + 15.5n$
[50]	4.1840	2.8387	2.3423	$20n^2 + 11n$
[32]	4.1821	3.1859	2.8905	$26.5n^2 + 16.5n$
[48]	4.1903	3.0779	2.8268	$66.5n^2 + 18.5n$
This paper	4.2102	3.1932	2.9572	$15.5n^2 + 11.5n$

are derived dependent on the development of appropriate L-K functional with DPT, and by utilizing recently presented integral inequality techniques (WSI, WDI), which increase the size of LMIS (9) and (10); as a result, some computational complexity can occur in the proposed criterion. It ought to be referenced that the acquired maximum allowable bounds (MABs) ρ are less conservative than the existing ones in the literature, it can be noted in Tables 2 and 3. As far the results to be efficient enough it is more comfortable to have MABs ρ but still in order to reduce computation complexity burden and time computation. Moreover, in the future studies we will focus on lower computational complexity of the stability problems while maintaining the desired system performances.

Remark 3.7. Note that Theorem 3.1 gives an adequate condition to co-plan the filter (3) and the event-triggered matrix $\hat{\Gamma}$. In addition, it can also be seen that the arrangement of system (7) depends not only on the lower and upper bounds of the neural network, but also on the upper bound of delay in communication channels, activated triggering parameters.

4. Simulation results

For clarifying the explanation of the proposed results, we will present an explained example in this part to validate the availability of the developed ETC law.

Example 4.1. Consider the RNNs (7) with the following parameters:

$$D = \begin{bmatrix} 5 & 0 \\ 0 & 4 \end{bmatrix}, \quad W1 = \begin{bmatrix} 1 & 0.4 \\ -2 & 0.1 \end{bmatrix}, \quad W_2 = \begin{bmatrix} 0.5 & 0.7 \\ 0.7 & 0.4 \end{bmatrix}, \quad W_3 = \begin{bmatrix} 0.5 & -0.3 \\ 0.2 & 1.2 \end{bmatrix},$$

It is easy to check that Assumption (H1) is satisfied, with $f_1(x) = tanh(0.7x) - 0.1sinx$, $f_2(x) = tanh(0.4x) + 0.2cosx$. It can be found that $G_1^- = -0.1, G_2^- = -0.2, G_1^+ = 0.8, G_2^+ = 0.6$. The time-delay upper bounds of ρ for different μ_1 and σ are calculated in Table 1. By utilizing the algorithm given below, numerical simulations have been performed on system parameters to validate the effectiveness of the proposed results.

(i) Select $\tau = 0.752$, $\mu_1 = 0.5$, $\sigma = 0.2$, $h = 0.2$, $c_1 = 2$, $c_2 = 5$, and $T = 8$.
(ii) Simply set the initial value of c_2, ρ and verify LMIs (26)–(27).
(iii) Suppose we get the infeasible solution, when solving the LMIs, mean time the value of c_2 could be ramping up and decreases the leakage term σ. Something else, decrease the value of c_2 until we get the essential value of feasible solutions.

Table 3
MABs ρ for various values of μ_1 in Example 4.5.

μ_1	0.8	0.9	NODVs
[17]	1.7792	1.6954	$60n^2 + 22n$
[32]	2.4812	2.4600	$26.5n^2 + 16.5n$
This paper	2.5201	2.4910	$15.5n^2 + 11.5n$

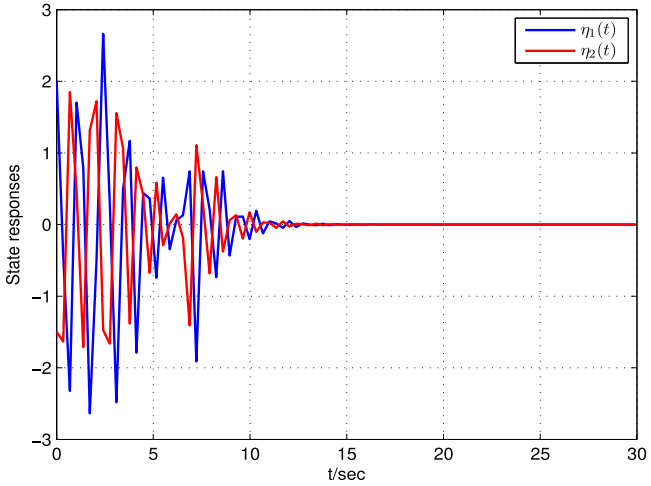

Fig. 2. Evolution of system state in Example 4.1 for $\sigma = 0.05$.

Moreover, by solving LMIs in Theorem 3.1 together with MATLAB LMI procedure, we get the feasible solutions which can be listed as follows:

$$P_1 = \begin{bmatrix} 46.2109 & -4.2472 \\ -4.2472 & 48.9617 \end{bmatrix}, \quad P_2 = \begin{bmatrix} 31.7441 & -0.3042v \\ -0.3042 & 31.2367 \end{bmatrix}, \quad P_3 = \begin{bmatrix} 9.6864 & 1.8941 \\ 1.8941 & 13.5448 \end{bmatrix},$$
$$P_4 = \begin{bmatrix} 0.2240 & -0.0149 \\ -0.0149 & 0.4083 \end{bmatrix}, \quad P_6 = \begin{bmatrix} 2.7640 & -0.0295 \\ -0.0295 & 3.4885 \end{bmatrix}, \quad P_7 = \begin{bmatrix} 95.7850 & -5.7439 \\ -5.7439 & 106.5625 \end{bmatrix},$$
$$P_8 = \begin{bmatrix} 0.4291 & -0.0262 \\ -0.0262 & 0.7517 \end{bmatrix}, \quad Q_1 = \begin{bmatrix} 4.8820 & -0.0401 \\ -0.0401 & 5.9536 \end{bmatrix}, \quad R_1 = \begin{bmatrix} 2.8729 & 0.3054 \\ 0.3054 & 3.7392 \end{bmatrix},$$
$$R_2 = \begin{bmatrix} 6.9950 & -0.8534 \\ -0.8534 & 15.5215 \end{bmatrix}, \quad V_1 = \begin{bmatrix} 0.8011 & -0.0575 \\ -0.0575 & 1.1774 \end{bmatrix}, \quad P = \begin{bmatrix} 25.3896 & -0.1254 \\ -0.1254 & 25.8535 \end{bmatrix}$$

Based on the solutions, the triggering parameters $\hat{\Gamma}$ and controller gain K can be respectively computed out as

$$\hat{\Gamma} = \begin{bmatrix} 33.2216 & -0.0516 \\ -0.0516 & 33.3679 \end{bmatrix}, \quad K = \begin{bmatrix} 0.5993 & -0.0510 \\ -0.0399 & 0.5277 \end{bmatrix}. \tag{34}$$

Under the initial states $[2, -1.5]^T$, the numerical illustrations of state trajectories $\eta_1(t)$, and $\eta_2(t)$ for the given system (7) are shown in Fig. 2. It ought to be referenced that, the maximum admissible value of leakage delay is 0.05 and $\rho(t) = 5.0203 + 0.1cos(t)$. Figs. 3–5 indicate the state trajectories for the delays $\rho(t) = 4.4681 + 0.1cos(t)$, $\rho(t) = 3.8672 + 0.1cos(t)$ and $\rho(t) = 3.0752 + 0.1cos(t)$ corresponding to 0.1, 0.15 and 0.2, respectively. Moreover, from Table 1, it can be easily verified that as leakage delay progressively increases, the calculated time-delay upper bounds of ρ get the infeasible value. Further, when $\sigma = 0.25$ the unstable behavior of the given system is predicted in Fig. 6. Fig. 7 exhibits the dynamical reaction of the control input. Additionally, the adequacy of results appeared through the simulation results of $\eta^T(t)\tilde{R}\eta(t)$ in Figs. 8 and 9. The initial conditions satisfy $\eta^T(0)\tilde{R}\eta(0) = c_1 = 0.9$

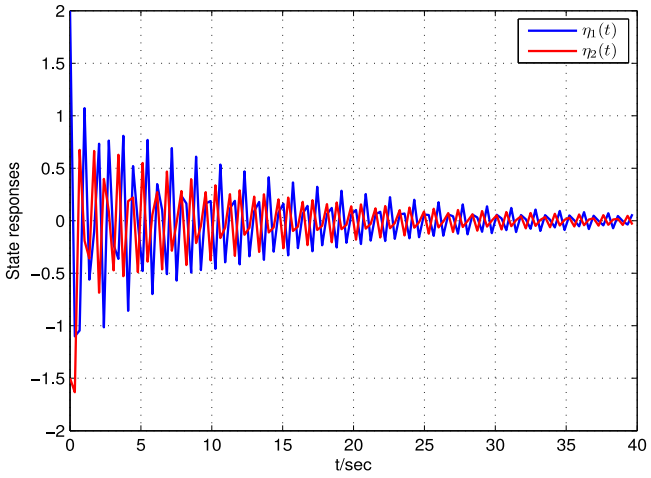

Fig. 3. Evolution of system state in Example 4.1 for $\sigma = 0.1$.

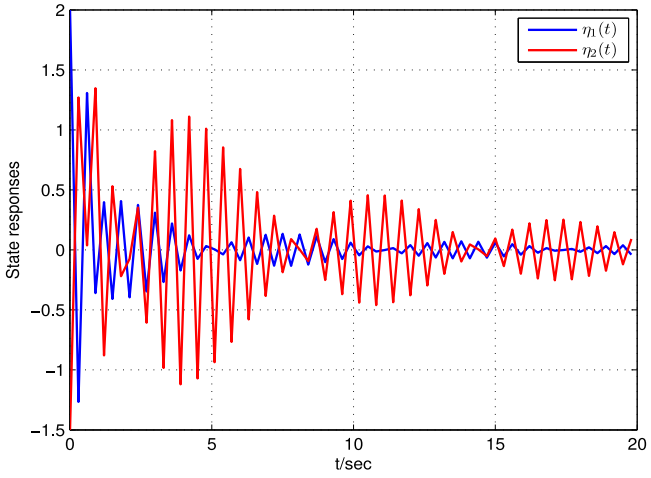

Fig. 4. Evolution of system state in Example 4.1 for $\sigma = 0.15$.

and the state trajectories of $\eta^T(t)\tilde{R}\eta(t) = c_2 = 8.5$. Henceforth, it can be reasoned that the proposed neural networks (7) are FTS. Notice that the system is stable as revealed by our theoretical results.

Example 4.2. Fundamentally, NNs show the propensity of certain biological neurons that have been associated or practically connected in a nervous system. Then again, NNs can be implemented together with biological neurons as well as a portion of the applicable models. One of them is the quadruple-tank process, which is depicted in Fig. 10. The quadruple-tank process comprises of four interconnected water tanks and two pumps. Along these (μ_1 *and* μ_2) denotes inputs voltages to the pumps 1 and 2, and the outputs are θ_1 and θ_2 (voltages from level estimation devices). As shown in Fig. 10, NN model utilizing the quadruple-tank process can be shown evidently. [14,15,19] suggested the state–space condition of the quadruple-tank process and developed the state feedback controller in the following way:

$$\dot{\eta}(t) = \tilde{\mathbf{A}}_0\eta(t) + \tilde{\mathbf{A}}_1 x(t-\hat{\rho}_1) + \tilde{B}_0 u(t-\hat{\rho}_2) + \tilde{\mathbf{B}}_1 u(t-\hat{\rho}_3), \tag{35}$$

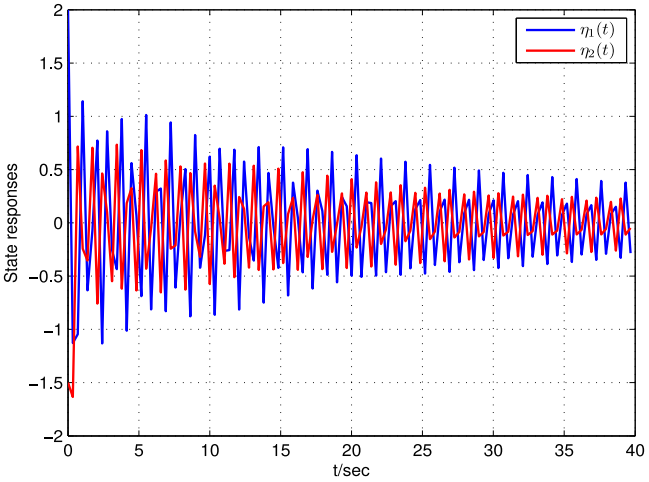

Fig. 5. Evolution of system state in Example 4.1 for $\sigma = 0.2$.

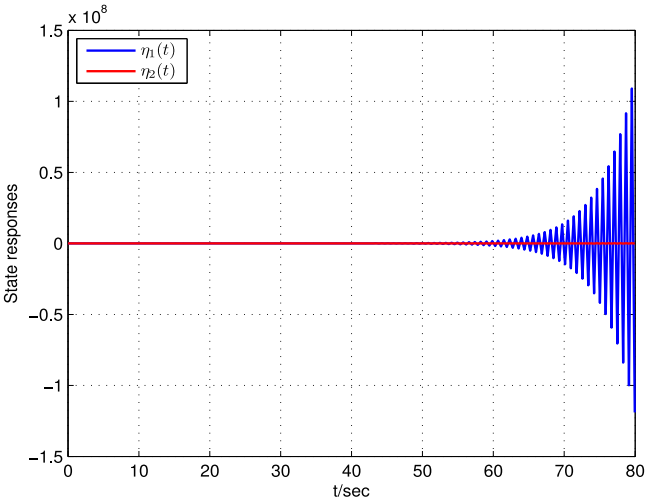

Fig. 6. Evolution of system state in Example 4.1 for $\sigma = 0.25$.

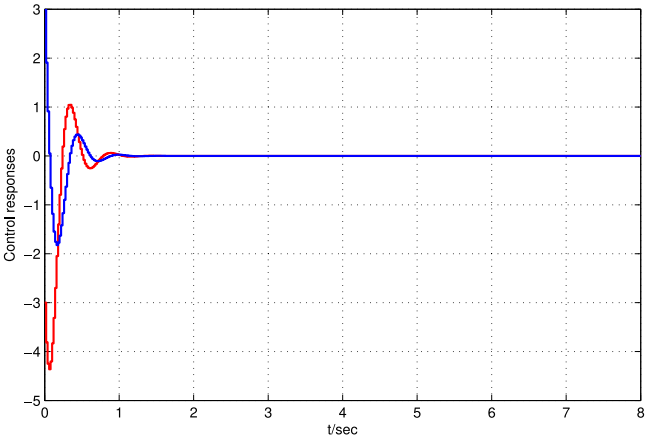

Fig. 7. Response of the control input in Example 4.1.

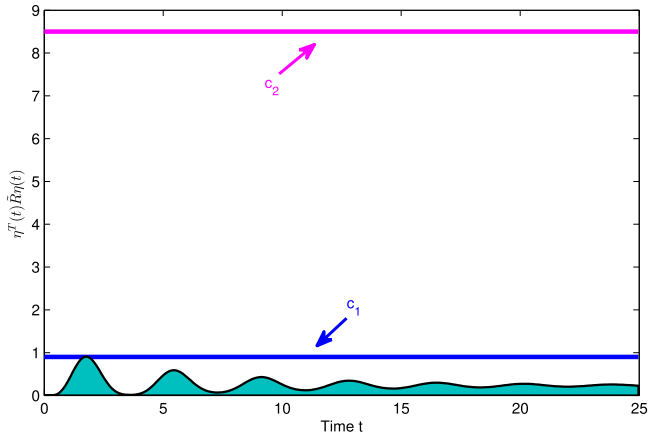

Fig. 8. State trajectory of $\eta^T(t)\tilde{R}\eta(t)$ in Example 4.1.

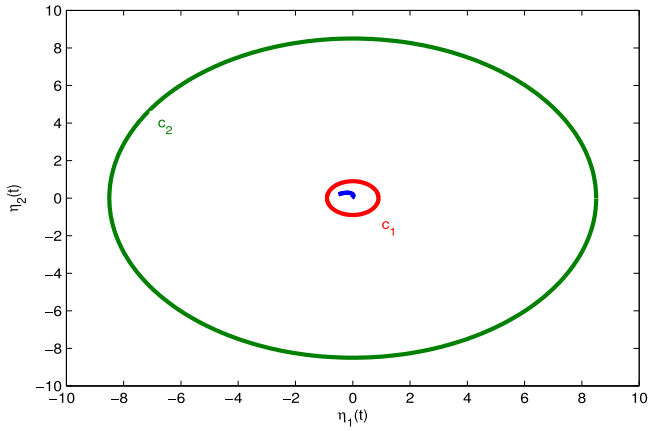

Fig. 9. Evolution of $\eta^T(t)\tilde{R}\eta(t)$ in Example 4.1.

where the parameters are given as follows:

$$\tilde{\mathbf{A}}_0 = \begin{bmatrix} -0.0021 & 0 & 0 & 0 \\ 0 & -0.0021 & 0 & 0 \\ 0 & 0 & -0.0424 & 0 \\ 0 & 0 & 0 & -0.0424 \end{bmatrix}, \quad \tilde{\mathbf{A}}_1 = \begin{bmatrix} 0 & 0 & 0.0424 & 0 \\ 0 & 0 & 0 & 0.0424 \\ 0 & 0 & 0 & 0 \\ 0 & 0 & 0 & 0 \end{bmatrix},$$

$$\tilde{\mathbf{B}}_0 = \begin{bmatrix} 0.1113\theta_1 & 0 & 0 & 0 \\ 0 & 0.1042\theta_2 & 0 & 0 \end{bmatrix}^T, \quad \tilde{\mathbf{B}}_1 = \begin{bmatrix} 0 & 0 & 0 & 0.1113(1-\theta_1) \\ 0 & 0 & 0.1042(1-\theta_2) & 0 \end{bmatrix}^T,$$

$$\tilde{K} = \begin{bmatrix} -0.1609 & -0.1765 & -0.0795 & -0.2073 \\ -0.1977 & -0.1579 & -0.2288 & -0.0772 \end{bmatrix}, \quad \theta_1 = 0.333, \ \theta_2 = 0.307, \ u(t) = \tilde{K}\tilde{x}(t).$$

Moreover, the transport delays within the tanks and valves change in terms of time-varying. In this regard the control issue, leakage delays can be tackled in QTPS (in terms of the water intake to the tanks) and are significant in our real life. For the simplicity, we pick both $\hat{\tau}_1 = \hat{\tau}_2$ are zero and $\hat{\tau}_3 = \rho(t)$. Since $u(t)$ thereby the quantity of water is provided by the pumps. Along these lines, it is normally a nonlinear function and can be represented in

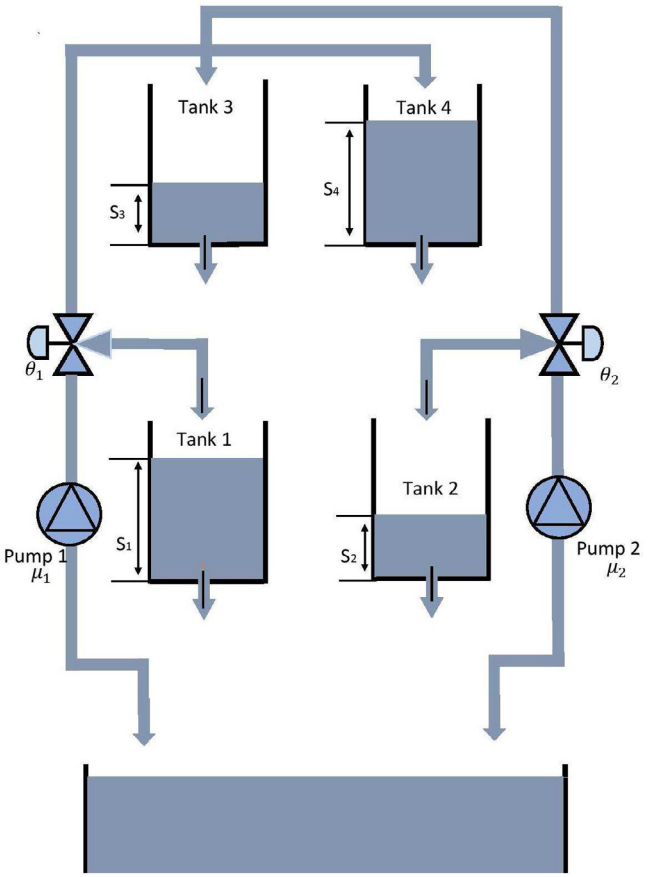

Fig. 10. Overview of the QTP model.
Source: From [15].

the following way:

$$u(t) = \tilde{K}\, g(\eta(t)),$$
$$g(\eta(t)) = [g_1(\eta(t)), \ldots, g_4(\eta(t))],$$
$$g_j(\eta_e(t)) = \frac{0.5}{5}(|\eta_j(t) + 1| - |\eta_j(t) - 1|),\ j = 1, 2, \ldots, 4.$$

The Quadruple-tank process (35) can be modeled in the following way:

$$\dot{\eta}(t) = -D\eta(t-\sigma) + W_1 f(\eta(t)) + W_2 f(\eta(t-\rho(t))), \tag{36}$$

where $D = -\tilde{\mathbf{A}}_0 - \tilde{\mathbf{A}}_1$, $W_1 = \tilde{\mathbf{B}}_0\tilde{K}$, $W_2 = \tilde{\mathbf{B}}_1\tilde{K}$, $f(\cdot) = g(\cdot)$. Furthermore, by taking the values $W_3 = [0\ 0\ 0\ 0]^T$, $G_1 = 0_4, G_2 = 0.1I_4, \mu_1 = 0.3$, $\rho = 0.5$, for various $\sigma = 0.1, 0.15, 0.2, 0.25, 0.3$ then the LMIs in Corollary 3.3, and we found that the QTPS (36) is FTS. Figs. 11–15 exhibit the state responses of the system converge to zero. From Figs. 11–15, it is clear that for a small amount of the leakage term the QTPS is actually stable. Suppose, if we increase the amount of the leakage term the state trajectories get some effects (because of the leakage term) thus reducing the system performance gradually, which can be shown in Figs. 16–18. Similarly, for leakage delay increases $\sigma = 0.35, 0.4, 0.5$, the state responses of the systems are divergences from the equilibrium point, these are represented in Figs. 16–18. In addition, time history of $\eta^T(t)\tilde{R}\eta(t)$ has been depicted in Fig. 19, a small amount of leakage term can keep the QTPS performance as stable and unstable for the large amount of leakage term. Thus, from the simulation results, it is guaranteed that leakage delay has a noteworthy impact on the QTPS.

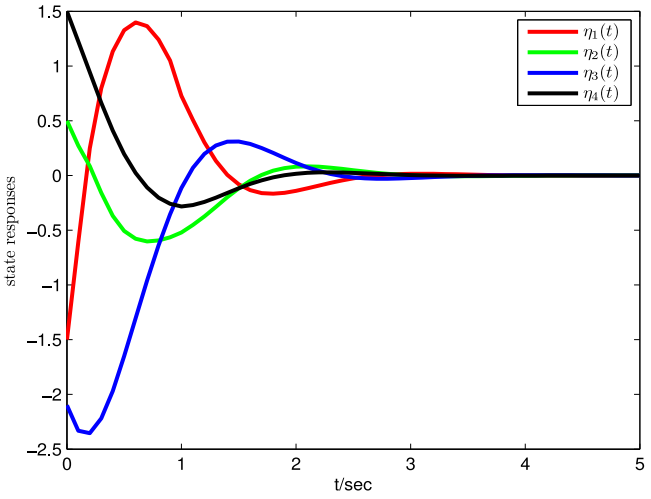

Fig. 11. Evolution of system state in Example 4.2 for $\sigma = 0.05$.

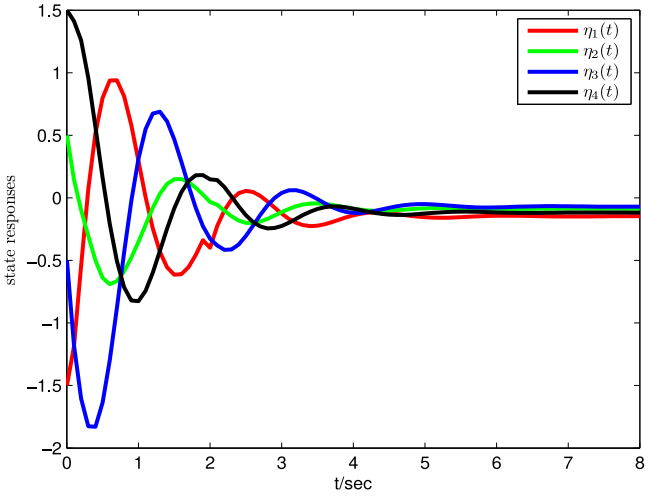

Fig. 12. Evolution of system state in Example 4.2 for $\sigma = 0.1$.

Example 4.3. A continuous-time artificial NN containing n units is described by the following differential equations [11]:

$$\begin{cases} \frac{d\eta_i(t)}{dt} = -\frac{\eta_i(t)}{R_i C_i} + \sum_{j=1}^{n} W_{ij} y_j(t) + u_i(t) \\ y_i(t) = f_i(\eta_i(t)) \end{cases} \tag{37}$$

In view of the results acquired in [11], system (37) can be executed by an analog resistance–capacitance network circuit (RCNC) as portrayed in Fig. 20, with

- η_i represents the input voltage of the i_{th} amplifier
- $V_i = f_i(\eta_i(t))$ signifies the output voltage of the ith amplifier, where every operational amplifier has double output terminals that are supplying V_i and $-V_i$.

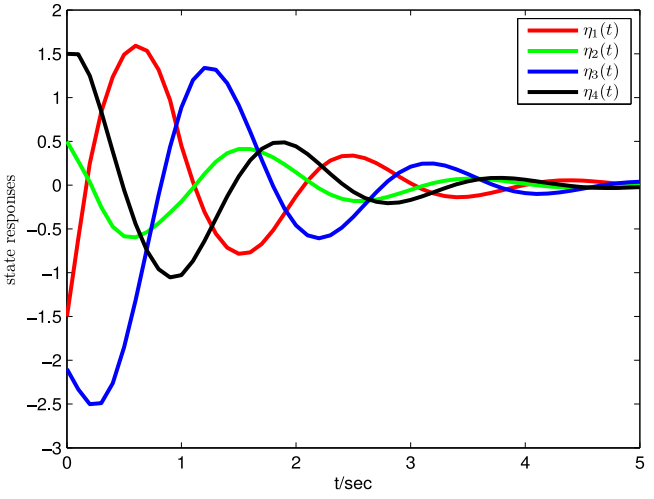

Fig. 13. Evolution of system state in Example 4.2 for $\sigma = 0.15$.

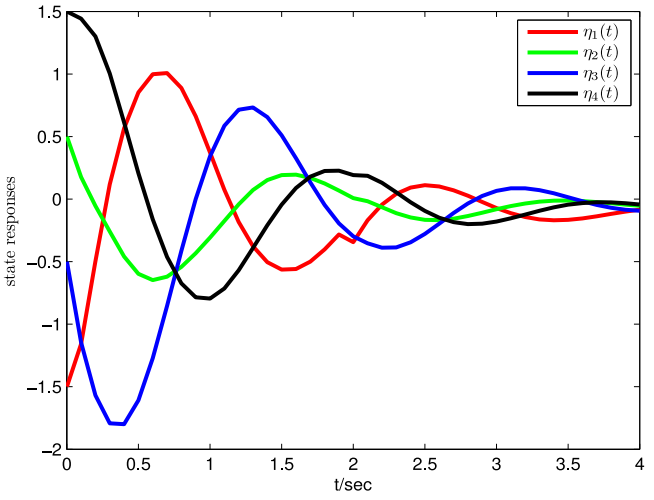

Fig. 14. Evolution of system state in Example 4.2 for $\sigma = 0.2$.

- R_i and the weight parameter w_{ij} are modeled in the following way:

$$\frac{1}{R_i} = \frac{1}{\sigma_i} + \sum_{j=1}^{n} \frac{1}{R_{ij}}$$

$$W_{ij} = \begin{cases} +\frac{1}{R_{ij}}, & R_{ij} \ is \ connected \ to \ V_j \\ -\frac{1}{R_{ij}}, & R_{ij} \ is \ connected \ to \ -V_j \end{cases}$$

Therefore, the system (37) can be rewritten as

$$\dot{\eta}(t) = -D\eta(t) + W_1 f(\eta(t)) + W_2 u \tag{38}$$

with

$$D = \begin{bmatrix} \frac{1}{R_1 C_1} & 0 \\ 0 & \frac{1}{R_2 C_2} \end{bmatrix}, W_1 = \begin{bmatrix} \frac{W_{11}}{C_1} & \frac{W_{12}}{C_1} \\ \frac{W_{21}}{C_2} & \frac{1}{\frac{W_{21}}{C_2}} \end{bmatrix}, W_2 = \begin{bmatrix} \frac{1}{C_1} & 0 \\ 0 & \frac{1}{C_2} \end{bmatrix}$$

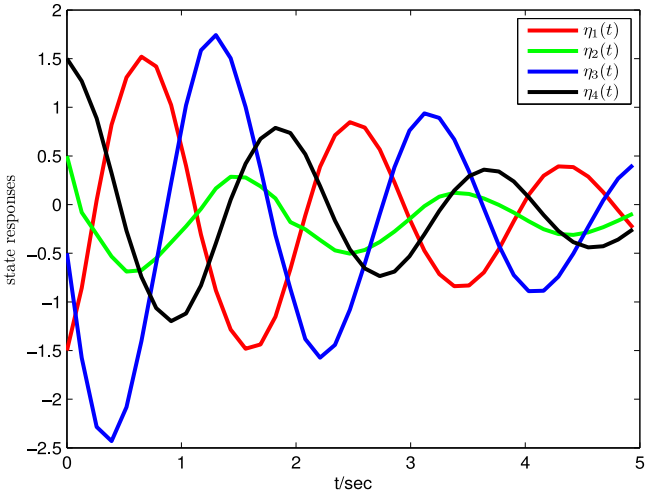

Fig. 15. Responses of the system state in Example 4.2 for $\sigma = 0.25$.

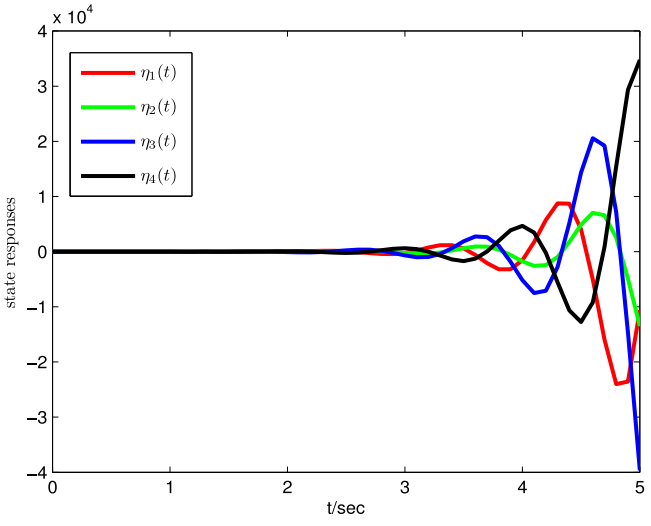

Fig. 16. Evolution of system state in Example 4.2 for $\sigma = 0.3$.

Time constant of the ith neuron has been depicted as $R_i C_i = \rho_i, i = 1, 2, \ldots, n$ and represenst the convergence of η_i. When $\rho_i = \rho$ for every neuron, each value for σ_i would have to be taken in such a way that it compensates for these variations and maintains R_i the same for every neuron. The output V_i may immerse rapidly because the transfer function has a very high gain of potentially. Consequently, even if η_i is still far to achieve its equilibrium, V_i may show up as though the circuit had converged in simply a small amount of ρ_i. Given the HDNNs outlined by (38) through the group of parameters:

$$R_i = C_i, \ i = 1, 2$$
$$W_1 = \begin{bmatrix} 1 & 1.5 \\ -1.5 & -1 \end{bmatrix}, \ f_i(t) = tanh(t),$$

which implies $G_1 = 0$, $G_2 = 0.5I$ and utilizing Matlab LMI toolbox and solving the LMIs in Corollary 3.3, a group of feasible solution can be acquired. Along these lines, it can be concluded that Corollary 3.3 infers that

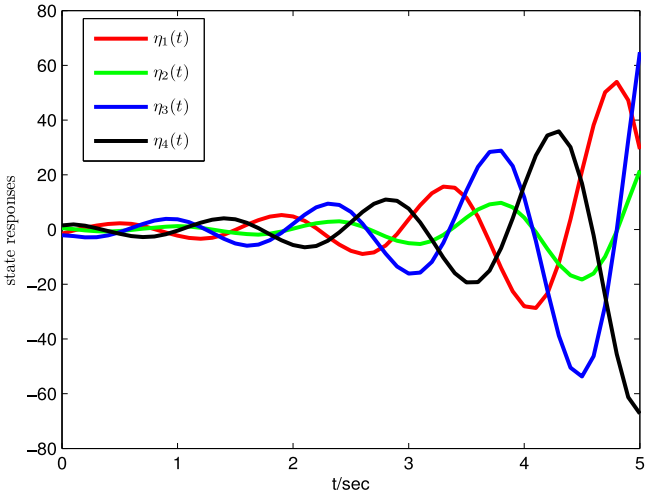

Fig. 17. Evolution of system state in Example 4.2 for $\sigma = 0.4$.

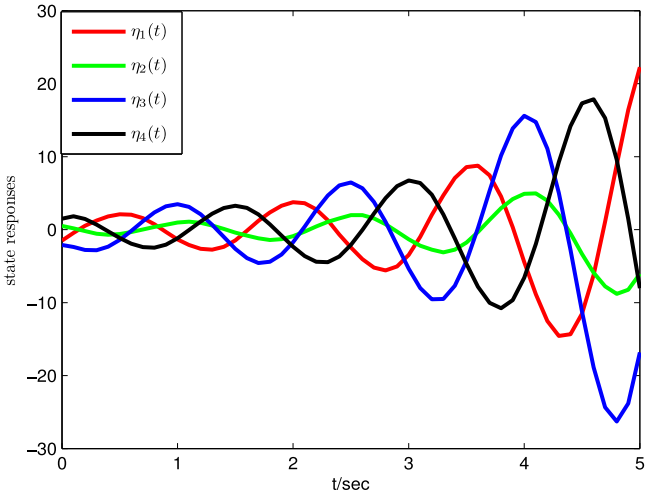

Fig. 18. Evolution of the system state in Example 4.2 for $\sigma = 0.5$.

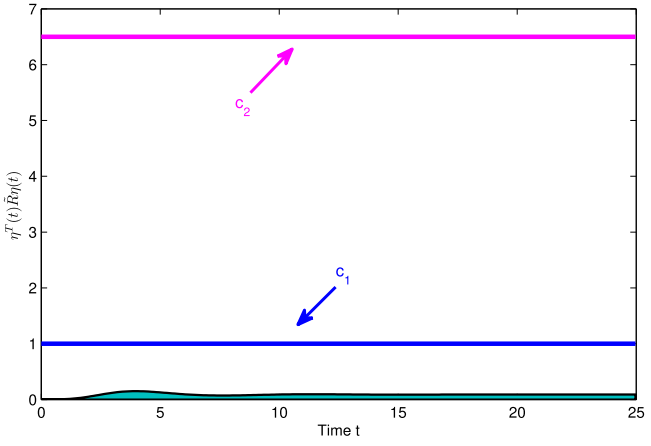

Fig. 19. State trajectory of $\eta^T(t)\tilde{R}\eta(t)$ in Example 4.2.

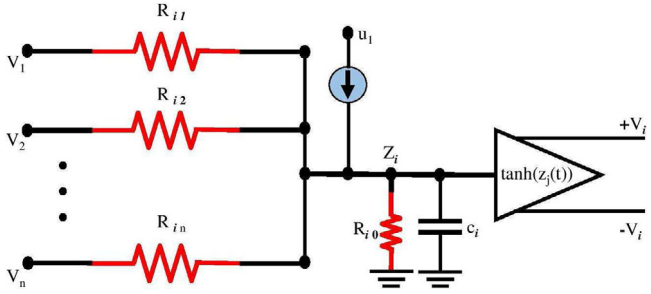

Fig. 20. Circuit for neuron i in the analog execution of Hopfield DNN.

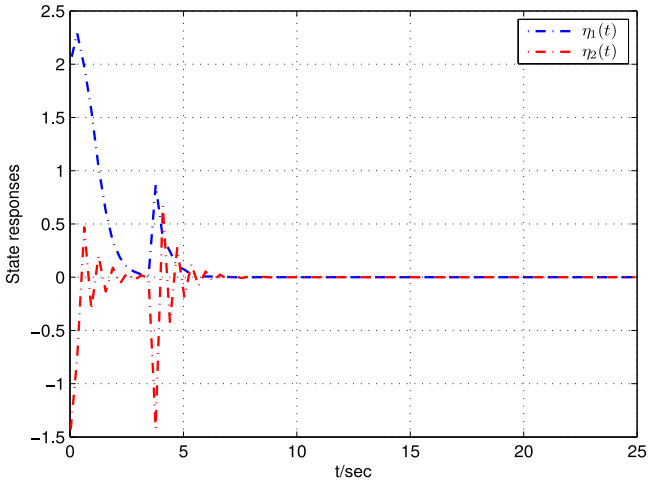

Fig. 21. Evolution of the system state in Example 4.3.

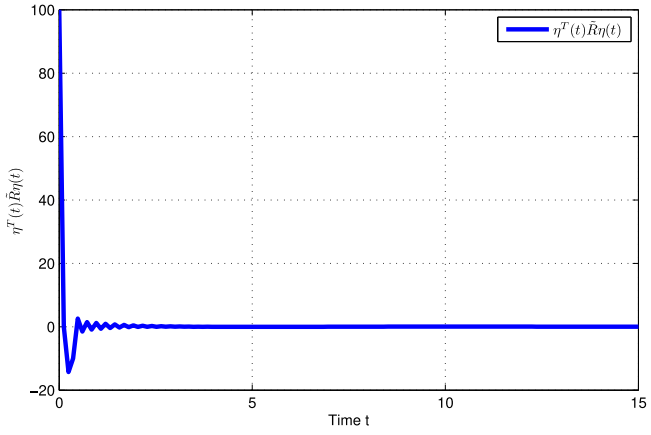

Fig. 22. Time history of $\eta^T(t)\tilde{R}\eta(t)$ for the system (38).

system (38) is finite time stable. The state responses of system (38) and responses of $\eta^T(t)\tilde{R}\eta(t)$ are shown in a row in Figs. 21 and 22 with the initial condition $\eta(s) = [2, -1.5]^T$.

Example 4.4. Consider the following four-neuron RNN system (31) with the matrix parameters in [30]:

$$D = diag\{1.7269,\ 0.6231,\ 0.9230,\ 0.4480\},\ W_1 = \begin{bmatrix} -0.0373 & 0.4852 & -0.3351 & 0.2336 \\ -1.6033 & 0.5988 & 0.3224 & 1.2352 \\ 0.3394 & -0.0860 & -0.3824 & -0.5785 \\ -0.1311 & 0.3253 & -0.9534 & -0.5015 \end{bmatrix},$$

$$W_2 = \begin{bmatrix} 0.8674 & -1.2405 & -0.5325 & 0.0220 \\ 0.0474 & -0.9164 & 0.0360 & 0.9816 \\ 1.8495 & 2.6117 & -0.3788 & 0.8428 \\ -2.0413 & 0.5179 & 1.1734 & -0.2775 \end{bmatrix},$$

$$G_2 = 0,\ G_1 = diag\{0.1137,\ 0.1279,\ 0.7994,\ 0.2368\}$$

Following the LMIs in Corollary 3.3 with $\sigma = 0$ choose the activation functions $f(x) = [0.0568(|\eta_1 + 1| - |\eta_1 - 1|), 0.0640(|\eta_2 + 1| - |\eta_2 - 1|), 0.3997(|\eta_3 + 1| - |\eta_3 - 1|), 0.1184(|\eta_4 + 1| - |\eta_4 - 1|)]^T$. For different values μ_1, the MABs ρ of $\rho(t)$ obtained by various methods are summarized in Table 2. From Table 2, clearly Corollary 3.3 provides larger MABs than those in [12,18,43,48,50], which suggests Corollary 3.3 in this paper is less conservative. Fig. 23 represents the state response of variables $\eta_1(t), \eta_2(t), \eta_3(t)$ and $\eta_4(t)$ for the system (31) with an initial condition $\eta(t) = [11.8, 1.5, -2.3, 0.5]^T$. The time history $\eta^T(t)\tilde{R}\eta(t)$ is provided in Fig. 24. In addition, it is worth pointing out that our stability criterion involves less number of decision variables (NODVs) than those in [12,18,43,48,50]. Therefore, with reference to Figs. 23, 24 and Table 2, it is evident that system (31) is FTS.

Example 4.5. Consider the following RNNs (31) with the matrix parameters in [32]:

$$D = diag\{1.1,\ 0.8,\ 0.7,\ 1.2,\ 1.2,\ 2\},$$

$$W_1 = \begin{bmatrix} 0.01 & 0 & -0.4 & 0 & 0.05 & 0 \\ 0.11 & 0 & -0.05 & 0 & 0.3 & 0 \\ 0.03 & 0 & -0.7 & 1.2 & 0.11 & 0 \\ 1.02 & 0 & -0.55 & 0.07 & 0.36 & 0 \\ 0.02 & 0.02 & -0.01 & -0.01 & -0.03 & 0 \\ 0.15 & 0.13 & 0 & 0 & -0.08 & 0.07 \end{bmatrix},$$

$$W_2 = \begin{bmatrix} 1.34 & -0.2 & 0.4 & 0.7 & -0.03 & 0.35 \\ -0.24 & 0.56 & 0.67 & -0.5 & 0.78 & -0.88 \\ 0.12 & 0.23 & 0.05 & -0.70 & 0.5 & 0 \\ 0.08 & 0.55 & -0.64 & 0.03 & 0.77 & 0.21 \\ 0.04 & 0.08 & 0.75 & 0.03 & 0.01 & 0.02 \\ 1.01 & 0.07 & 0.08 & 0.32 & 0.14 & -0.02 \end{bmatrix},$$

$$G_2 = 0,\ G_1 = diag\{0.5,\ 0.5,\ 0.5,\ 0.4,\ 0.4,\ 0.4\}.$$

By solving Example 4.5 utilizing LMIs in Corollary 4.5 with $\sigma = 0$, we get MABs ρ of $\rho(t)$ obtained by the method in [17,32] and Corollary 3.3 in this paper is given in Table 3. Table 3 shows Corollary 3.3 is less conservative than in Refs [17] and [32]. The NODVs required in Theorem 1 in [17] are $60n^2+22n$, Corollary 1 in [32] is $26.5n^2+16.5n$ and Corollary 3.3 in this paper just requires $15.5n^2+11.5n$ decision variables, which clearly shows the effectiveness of our work.

5. Conclusion

Finite time stability analysis has been discussed for event triggered RNNs with time-varying delay and leakage terms, so as to demonstrate the FTS of the proposed system, lot of techniques such as the method of WSI, WDI technique, DPT, Lyapunov stability theory, and Jensen inequality approaches have been effectively utilized in this

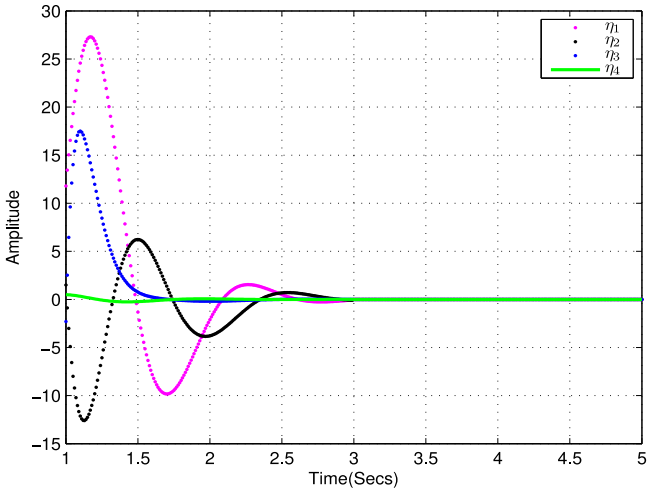

Fig. 23. State trajectory of system (31) with $\sigma = 0$ in Example 4.4.

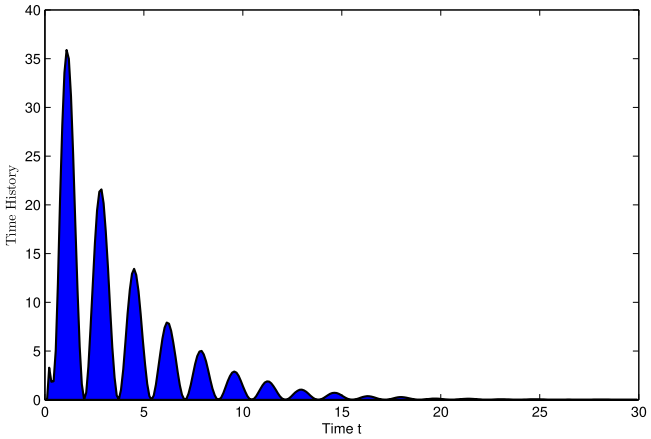

Fig. 24. Time history of $\eta^T(t)\tilde{R}\eta(t)$.

work, which are stated with respect to LMIs to show the feasibility of this paper. At last, to exhibit the adequacy of the proposed results, standard numerical examples are examined with real life application problems. In the future, it is an interesting task to extend the proposed method for dealing with some practical systems, such as offshore platforms, multi-robot formation control systems, multi-agent systems, load frequency control systems, coupled neural networks with imperfect communication, such as packet dropouts and quantization and PMSM model, which makes the model more practical. We will also concentrate on the discrete time matters for the networked control system and finite time issues for networked control switched system under an improved ETS are additional goals for the further investigation.

References

[1] C.K. Ahn, State estimation for T-S fuzzy Hopfield neural networks via strict output passivation of the error system, Int. J. Gen. Syst. 42 (2013) 503–518.

[2] F. Amato, R. Ambrosino, M. Ariola, C. Cosentino, G.D. Tommasi, Finite-Time Stability and Control, Springer, London, 2014.

[3] R. Baranitha, R. Rakkiyappan, R. Mohajerpoor, S. Al-Wais, Stability analysis of nonlinear telerobotic systems with time-varying communication channel delays using general integral inequalities, Inform. Sci. 465 (2018) 353–372.

[4] Y. Cao, S. Wang, Z. Guo, T. Huang, S. Wen, Synchronization of memristive neural networks with leakage delay and parameters mismatch via event-triggered control, Neural Netw. 119 (2019) 178–189.

[5] Z. Chen, B. Liu, Convergence behavior of Cohen-Grossberg neural networks with time-varying delays in the leakage terms, Neurocomputing 120 (2013) 518–523.
[6] M. Dai, J. Xia, H. Xia, H. Shen, Event-triggered passive synchronization for Markov jump neural networks subject to randomly occurring gain variations, Neurocomputing 331 (2019) 403–411.
[7] Y. Fan, X. Huang, H. Shen, J. Cao, Switching event-triggered control for global stabilization of delayed memristive neural networks: an exponential attenuation scheme, Neural Netw. 117 (2019) 216–224.
[8] E. Garcia, Y. Cao, D. Wellman Casbeer, Decentralized event-triggered consensus with general linear dynamics, Inform. Sci. 50 (2014) 2633–2640.
[9] K. Gopalsamy, Stability and Oscillations in Delay Differential Equations of Population Dynamics, Kluwer, Dordrecht, 1992.
[10] K. Gopalsamy, Leakage delays in BAM, J. Math. Anal. Appl. 325 (2007) 1117–1132.
[11] M. Gupta, L. Jin, N. Homma, Static and Dynamic Neural Networks: From Fundamentals to Advanced Theory, WileyIEEE Press, 2013.
[12] Y. He, G. Liu, D. Rees, New delay-dependent stability criteria for neural networks with time-varying delay, IEEE Trans. Neural. Netw. 18 (2007) 310–314.
[13] Ju. H.Park, C.H. Park, O.M. Kwon, S.M. Lee, A new stability criterion for bidirectional associative memory neural networks of neutral-type, Neurocomputing 199 (2008) 716–722.
[14] T. Huang, C. Li, S. Duan, J.A. Starzyk, Robust exponential stability of uncertain delayed neural networks with stochastic perturbation and impulse effects, IEEE Trans. Neural Netw. Learn. Syst. 23 (2012) 866–875.
[15] K.H. Johansson, The quadruple-tank process: a multivariable laboratory process with an adjustable zero, IEEE Trans. Control Syst. Technol. 8 (2000) 456–465.
[16] B. Kosko, Neural Networks and Fuzzy Systems, Prentice Hall, New Delhi, 1992.
[17] O.M. Kwon, S.M. Lee, Ju. H. Park, E.J. Cha, New approaches on stability criteria for neural networks with interval time-varying delays, Appl. Math. Comput. 218 (2012) 9953–9964.
[18] O.M. Kwon, Ju. H. Park, S.M. Lee, E.J. Cha, Analysis on delay-dependent stability for neural networks with time-varying delays, Neurocomputing 103 (2013) 114–120.
[19] T.H. Lee, Ju. H. Park, O.M. Kwon, S.M. Lee, Stochastic sampled-data control for state estimation of time-varying delayed neural networks, Neural Netw. 46 (2013) 99–108.
[20] P. Lee, Y. Lee, D. Cheng, X. Liu, Steady-state analysis of an interleaved boost converter with coupled inductors, IEEE Trans. Ind. Electron. 47 (2000) 787–795.
[21] C. Li, T. Huang, On the stability of nonlinear systems with leakage delay, J. Franklin Inst. 346 (2009) 366–377.
[22] P. Liu, New results on delay-range-dependent stability analysis for interval time-varying delay systems with non-linear perturbations, ISA Trans. 57 (2015) 93–100.
[23] D. Liu, F. Hao, Decentralized event-triggered control strategy in distributed networked systems with delays, Int. J. Control. Autom. 11 (2013) 33–40.
[24] Y. Liu, B. Shen, H. Shu, Finite-time resilient H_∞ state estimation for discrete-time delayed neural networks under dynamic event-triggered mechanism, Neural Netw. 121 (2020) 356–365.
[25] S. Long, Q. Song, X. Wang, D. Li, Stability analysis of fuzzy cellular neural networks with time delay in the leakage term and impulsive perturbations, J. Franklin Inst. 349 (2012) 2461–2479.
[26] W. Lu, R. Zheng, T. Chen, Centralized and decentralized global outer-synchronization of asymmetric recurrent time-varying neural network by data-sampling, Neural Netw. 75 (2014) 22–31.
[27] M. Luo, S. Zhong, J. Cheng, Finite-time event-triggered control and fault detection for singular Markovian jump mixed delay systems under asynchronous switching, Adv. Differential Equations 80 (2018) http://dx.doi.org/10.1186/s13662-018-1533-y.
[28] R. Manivannan, S. Panda, K.T. Chong, J. Cao, An Arcak-type state estimation design for time-delayed static neural networks with leakage term based on unified criteria, Neural Netw. 106 (2018) 110–126.
[29] M. Maz, P. Tabuada, Decentralized event-triggered control over wireless sensor/actuator networks, IEEE Trans. Automat. Control 56 (2011) 2456–2461.
[30] P. Muthukumar, K. Subramanian, S. Lakshmanan, Robust finite time stabilization analysis for uncertain neural networks with leakage delay and probabilistic time-varying delays, J. Franklin Inst. 353 (2016) 4091–4113.
[31] M.J. Park, O.M. Kwon, J.H. Park, S.M. Lee, E.J. Cha, Stability of time-delay systems via Wirtinger-based double integral inequality, Automatica 55 (2015) 204–208.
[32] S. Qiu, X. Liu, F. Wang, Y. Shu, Robust stability analysis for uncertain recurrent neural networks with leakage delay based on delay-partitioning approach, Neural. Comput. Appl. 30 (2018) 211–222.
[33] R. Rakkiyappan, K. Maheswari, K. Sivaranjani, Y.H. Joo, Non-fragile finite-time $l_2 - l_\infty$ state estimation for discrete-time neural networks with semi-Markovian switching and random sensor delays based on Abel lemma approach, Nonlinear Anal. Hybrid Syst. 29 (2018) 283–302.
[34] R. Rakkiyappan, R. Sasirekha, Y. Zhu, L. Zhang, H_∞ state estimator design for discrete-time switched neural networks with multiple missing measurements and sojourn probabilities, J. Franklin Inst. 353 (2016) 1358–1385.
[35] H. Ren, G. Zong, C.K. Ahn, Event-triggered finite-time resilient control for switched systems: an observer-based approach and its applications to a boost converter circuit system model, Nonlinear Dynam. 94 (2018) 2409–2421.
[36] A. Seuret, F. Gouaisbaut, Wirtinger-based integral inequality: Application to time-delay systems, Automatica 49 (2013) 2860–2866.
[37] K. Sivaranjani, R. Rakkiyappan, Pinning sampled-data synchronization of complex dynamical networks with Markovian jumping and mixed delays using multiple integral approach, Complexity 21 (2016) 622–632.
[38] Q. Song, J. Cao, Passivity of uncertain neural networks with both leakage delay and time-varying delay, Nonlinear Dynam. 67 (2012) 1695–1707.

[39] M. Syed Ali, Stability of Markovian jumping recurrent neural networks with discrete and distributed time-varying delays, Neurocomputing 149 (2015) 1280–1285.
[40] P. Tallapragada, N. Chopra, Decentralized event-triggering for control of nonlinear systems, IEEE Trans. Automat. Control 59 (2014) 3312–3324.
[41] Y. Tong, D. Tong, Q. Chen, Finite-time state estimation for nonlinear systems based on event-triggered mechanism, Circuits Syst. Signal Process. (2020) http://dx.doi.org/10.1007/s00034-019-01334-4.
[42] A. Wang, T. Dong, X. Liao, Event-triggered exponential synchronization for complex-valued memristive neural networks with time-varying delays, IEEE Trans. Neural Netw. Learn. Syst. (2019) http://dx.doi.org/10.1109/TNNLS.2019.2952186.
[43] Z.S. Wang, L. Liu, Q.H. Shan, H. Zhang, Stability criteria for recurrent neural networks with time-varying delay based on secondary delay partitioning method, IEEE Trans. Neural Netw. Learn Syst. 26 (2015) 2589–2595.
[44] X. Wang, Z. Wang, Q. Song, H. Shen, X. Huang, A waiting-time-based event-triggered scheme for stabilization of complex-valued neural networks, Neural Netw. 121 (2020) 329–338.
[45] L. Xiaoxiao, R. Rakkiyappan, X. Li, μ-stability criteria for nonlinear differential systems with additive leakage and transmission time-varying delays, Nonlinear Anal. Model. Control 23 (2018) 380–400.
[46] H. Yan, H. Zhang, X. Zhan, Y. Wang, S. Chen, F. Yang, Event-triggered sliding mode control of switched neural networks with mode-dependent average dwell time, IEEE Trans. Syst. Man, Cybern. Syst. (2019) http://dx.doi.org/10.1109/TSMC.2019.2894984.
[47] H. Zeng, Y. He, M. Wu, J. She, New results on stability analysis for systems with discrete distributed delay, Automatica 60 (2015) 189192.
[48] H.B. Zeng, Y. He, M. Wu, S.P. Xiao, Stability analysis of generalized neural networks with time-varying delays via a new integral inequality, Neurocomputing 161 (2015) 148–154.
[49] J. Zhang, C. Peng, Synchronization of master–slave neural networks with a decentralized even triggered communication scheme, Neurocomputing 173 (2016) 1824–1831.
[50] X. Zhou, J. Tian, H. Ma, S. Zhong, Improved delay-dependent stability criteria for recurrent neural networks with time-varying delays, Neurocomputing 129 (2014) 401–408.